

# Unified Optimization of Source Weights and Transfer Quantities in Multi-Source Transfer Learning: An Asymptotic Framework

Qingyue Zhang, Chang Chu, Haohao Fu, Tianren Peng, Yanru Wu, Guanbo Huang, Yang Li, and Shao-Lun Huang

**Abstract**—Transfer learning plays a vital role in improving model performance in data-scarce scenarios. However, naive uniform transfer from multiple source tasks may result in negative transfer, highlighting the need to properly balance the contributions of heterogeneous sources. Moreover, existing transfer learning methods typically focus on optimizing either the source weights or the amount of transferred samples, while largely neglecting the joint consideration of the other. In this work, we propose a theoretical framework, Unified Optimization of Weights and Quantities (UOWQ), which formulates multi-source transfer learning as a parameter estimation problem grounded in an asymptotic analysis of a Kullback–Leibler divergence-based generalization error measure. The proposed framework jointly determines the optimal source weights and optimal transfer quantities for each source task. Firstly, we prove that using all available source samples is always optimal once the weights are properly adjusted, and we provide a theoretical explanation for this phenomenon. Moreover, to determine the optimal transfer weights, our analysis yields closed-form solutions in the single-source setting and develops a convex optimization-based numerical procedure for the multi-source case.

Building on the theoretical results, we further propose practical algorithms for both multi-source transfer learning and multi-task learning settings. Extensive experiments on real-world benchmarks, including DomainNet and Office-Home, demonstrate that UOWQ consistently outperforms strong baselines. The results validate both the theoretical predictions and the practical effectiveness of our framework.

**Index Terms**—transfer learning, multi-source learning, asymptotic analysis, K-L divergence,

## I. INTRODUCTION

Transfer learning has emerged as a critical paradigm in modern machine learning, especially in scenarios where labeled data is scarce for the target task. By leveraging knowledge from related source tasks, transfer learning enables models to generalize more effectively and efficiently to the target task. In recent years, transfer learning has a wide range of applications. For example, in deep reinforcement learning, transfer learning plays a crucial role in accelerating policy learning and improving sample efficiency by transferring policies, representations, or experience [1]. In healthcare, transfer learning leverages large medical datasets to support rare disease diagnosis with

The authors are with the Tsinghua Shenzhen International Graduate School, Tsinghua University, Shenzhen, China.

This work was supported in part by the National Key R&D Program of China under Grant 2021YFA0715202, the National Natural Science Foundation of China under Grants 62571296, and the Shenzhen Science and Technology Program under Grant KJZD20240903102700001.

Corresponding authors: Yang Li (yangli@sz.tsinghua.edu.cn), Shao-Lun Huang (twn2gold@gmail.com).

limited clinical data [2]. In natural language processing, pre-trained models built on large-scale transfer learning foundations have revolutionized performance across a wide range of downstream tasks [3]. While single-source transfer learning has been studied earlier, growing attention is now being paid to the multi-source transfer learning. In such scenarios, one key question is how to effectively use the data from the source tasks. For tasks that share more similarity with the target, its samples ought to be used more extensively, while for tasks that are less similar, its samples should be used with caution. In fact, transferred knowledge can even undermine the learning of target task, which is termed as negative transfer.[4] In multi-source transfer learning scenarios where source data are considered to be abundant with respect to target data, it is important to determine the effective amount of information to be transferred.

From a statistical perspective, while leveraging additional data from source tasks can reduce estimation variance and improve generalization, heterogeneity between source and target tasks may introduce systematic bias, resulting in negative transfer. Moreover, in multi-source settings, different source tasks often exhibit substantially different levels of relevance to the target task, making effective transfer learning non-trivial. Existing approaches typically address this challenge from one of two separate perspectives. On the one hand, task- or source-weighting methods aim to control the influence of different sources by assigning importance weights, thereby mitigating bias caused by irrelevant or mismatched domains. In current research on task weighting, most existing methods focus on assigning weights to source models, while relatively few studies assign weights to samples for unified learning. Moreover, existing weighting frameworks typically assume that all source samples are utilized by default. On the other hand, sample selection methods address the problem of deriving the optimal transfer quantity and selecting the identity of source samples to be transferred. Considering source weighting and transfer quantity in isolation restricts the solution space and can lead to suboptimal solutions, whereas jointly optimizing them leads to more principled and effective solutions. The goal of this work is to establish a theoretical framework that determines both the optimal source weights and transfer quantities, which are directly assigned to individual samples for joint training. In Table I, we provide a detailed comparison of the proposed method with several existing methods.

In this work, we develop a theoretical framework termed

TABLE I

**COMPARISON ACROSS MATCHING-BASED TRANSFER LEARNING METHODS**, BASED ON WHETHER THEY PERFORM QUANTITY OPTIMIZATION, WEIGHT OPTIMIZATION, ARE TAILORED TO MULTI-SOURCES, HAVE TASK GENERALITY, HAVE SHOT GENERALITY, AND REQUIRE TARGET LABELS. THE ‘✓’ REPRESENTS OBTAINING THE CORRESPONDING ASPECTS, WHILE ‘✗’ REPRESENTS THE OPPOSITE. QUANTITY OPTIMIZATION DENOTES THE ABILITY TO DETERMINE HOW MANY SOURCE SAMPLES OR DATA SUBSETS SHOULD BE TRANSFERRED. WEIGHT OPTIMIZATION DENOTES THE ABILITY TO ASSIGN OR LEARN WEIGHTS FOR DIFFERENT SOURCE TASKS OR SAMPLES. TASK GENERALITY DENOTES THE ABILITY TO HANDLE VARIOUS TARGET TASK TYPES, AND SHOT GENERALITY DENOTES THE ABILITY TO AVOID NEGATIVE TRANSFER IN DIFFERENT TARGET SAMPLE QUANTITY SETTINGS, INCLUDING FEW-SHOT AND NON-FEW-SHOT.

Method	Quantity Optimization	Weight Optimization	Multi-Source	Task Generality	Shot Generality	Target Label
MCW [5]	✗	✓	✓	✗	✗	Supervised
Leep [6]	✗	✗	✗	✓	✓	Supervised
Tong [7]	✗	✓	✓	✗	✓	Supervised
DATE [8]	✗	✓	✓	✓	✓	Unsupervised
H-ensemble [9]	✗	✓	✓	✗	✗	Supervised
FOMA [10]	✓	✗	✓	✗	✗	Supervised
DBF [11]	✓	✗	✗	✗	✗	Supervised
OTQMS [9]	✓	✗	✓	✓	✓	Supervised
UOWQ (Ours)	✓	✓	✓	✓	✓	Supervised

**Unified Optimization of Weights and Quantities (UOWQ)**, to determine the optimal weights and quantities for source tasks in transfer learning via asymptotic analysis. Using the measure based on Kullback–Leibler (K-L) divergence, we formulate the multi-source transfer learning problem as a parameter estimation problem, which in turn derives an optimization problem of the source weights and transfer quantities. We address this problem through an asymptotic analysis, which leads to the conclusion that using all available source samples is always optimal once the weights are properly adjusted, and further provides a principled method to calculate the optimal source weights. Specifically, to determine the optimal transfer weight, our analysis provides closed-form solutions in the single-source case and develops a convex-optimization-based numerical procedure in the multi-source case. Furthermore, we investigate why using all samples remains optimal under the joint optimization of weights and quantities, and analyze how the optimal weights are influenced by domain discrepancy, model dimensionality, and sample size. Moreover, we introduce practical algorithms capable of supporting both multi-source transfer learning and multi-task transfer learning. Finally, we validate the effectiveness of our proposed method through experiments on real-world dataset.

The main contributions of this work are summarized as follows:

- **Theoretical framework.** We introduce a mathematical framework, UOWQ, which formulates multi-source transfer learning as a parameter estimation problem and grounds it in an asymptotic analysis of a Kullback–Leibler divergence-based generalization error measure. The analysis yields closed-form solutions for the optimal transfer quantity and the optimal transfer weight in the single-source case, and proposes a convex-optimization-based solution method for the multi-source case. In particular, it provides a theoretical proof and interpretation for the fact that using all source samples is always optimal under the derived conditions.
- **Practical algorithm.** We develop a practical weighting algorithm derived from the theory, which assigns sample-

level source weights and can be directly applied to both multi-source transfer learning and multi-task learning. To cope with scarce target data and ensure robustness, the weights are updated dynamically during training. Specifically, the algorithms alternate between model optimization and source weight updates. At each stage, the model is trained using target data together with adaptively weighted source samples, while the source weights are updated based on the parameters of the current model state. This iterative procedure jointly refines the target model and the transfer strategy, and naturally extends to both learning scenarios.

- **Experimental validation.** We perform extensive experiments on the DomainNet and Office–Home benchmarks under both multi-source transfer learning and multi-task learning settings. In the 10-shot multi-source transfer scenario, UOWQ consistently outperforms strong baselines, achieving average accuracy improvements of 1.3% on DomainNet and 1.4% on Office–Home. Moreover, in the multi-task learning setting, UOWQ surpasses state-of-the-art task-weighting methods by 0.7% on DomainNet and 0.4% on Office–Home in terms of overall average performance. In addition, we conduct comprehensive ablation and robustness studies, including analyses under varying target-shot regimes, weight visualization, and computational efficiency evaluations, to further validate the theoretical insights and practical robustness of UOWQ.

This work is an extension of our previous conference paper [12], and the additional contributions are summarized as follows. First, the journal version unifies the optimization of both the optimal transfer quantities and the optimal source weights, and provides the complete theoretical proofs. Second, we include new theoretical analyses, including comparisons with related theoretical frameworks and an explanation of why maximizing the total transfer quantity remains optimal under joint optimization. Third, on the algorithmic side, we extend the multi-source method to a full multi-task learning algorithm. Finally, the experimental section is substantially

strengthened, covering larger datasets, more baselines, and extensive supplementary experiments, including ablation studies, robustness evaluations, analyses of computational efficiency, and compatibility with LoRA (Low-Rank Adaptation).

The remainder of this paper is organized as follows. Section II reviews the related work. Section III presents the problem formulation and introduces the asymptotic normality of the maximum likelihood estimator (MLE). Section IV develops the main theoretical results for computing the optimal source weights and introduces the practical algorithm. Section V empirically evaluates the proposed framework and validates the theoretical findings.

## II. RELATED WORK

### A. Multi-source Transfer Learning

Multi-source transfer learning (MSTL) leverages knowledge from multiple related source domains or tasks to improve performance on a target task, addressing challenges such as domain shift and negative transfer. Unlike single-source transfer, MSTL integrates diverse source knowledge through dynamic source weighting [13], shared feature space alignment [14], and ensemble- or meta-learning-based aggregation [15]. By emphasizing relevant sources while suppressing less informative ones, MSTL enhances generalization in heterogeneous settings, where effective learning requires balancing source contributions and mitigating distribution discrepancies.

From the perspective of the *transfer object*, multi-source transfer learning methods can be broadly categorized into **model-based** and **sample-based** transfer [16]. Model-based approaches leverage pretrained source models through fine-tuning or parameter adaptation [17], whereas sample-based methods jointly train on target and weighted source samples, enabling more direct exploitation of task-relevant source data [18–20].

From the perspective of the *transfer strategy*, existing methods can be further divided into **alignment-based** and **matching-based** approaches [21]. Alignment-based methods reduce domain discrepancy by explicitly aligning feature distributions [20, 22, 23], while matching-based methods emphasize informative sources or samples via selective weighting [7, 9, 19, 24]. Our method is more closely aligned with the **sample-based, matching-based** category, as it adopts a unified framework that jointly optimizes transfer quantities and source weights for weighted joint training.

### B. Task weighting

Task weighting, also referred to as source weighting, is a representative class of **matching-based** approaches in multi-source transfer learning and multi-task learning (MTL), as it regulates the contribution of different tasks without explicitly aligning feature distributions. Its objective is to balance competing task objectives during joint optimization. Early approaches relied on **static weighting**, assigning fixed weights based on heuristics such as task priority or dataset size [25], but these methods lack adaptability to dynamic task interactions. Recent studies have therefore focused on **dynamic**

**task weighting** strategies. For example, uncertainty-based weighting was introduced in [26], GradNorm balances tasks by normalizing gradient magnitudes [27], and DWA adjusts weights according to task learning speeds [28]. From a multi-objective optimization perspective, MGDA [29] formulates task weighting as a Pareto-optimal optimization problem.

Recent work has further extended task weighting to large-scale pretrained models, primarily through gradient-based matching mechanisms. For instance, [30] reweights tasks via gradient alignment, while [31] proposes **CAGrad** to mitigate conflicting gradients. Other studies explore **meta-learning**-based strategies [32] and task affinity to automate weighting. Despite these advances, task weighting remains challenged by nonstationary task relationships [33], scalability to large task sets, and the lack of strong theoretical guarantees [34, 35]. Benchmark datasets such as **Meta-Dataset** [36] have been introduced to facilitate standardized evaluation.

Most existing task-weighting methods operate at the model level, assigning scalar weights to source models in a mixture-of-experts fashion [37]. These approaches typically rely on task similarity [38], domain divergence [39], or validation performance [40]. In contrast, only a limited number of studies consider *sample-level* weighting, where source samples are reweighted and jointly trained with the target data in a unified framework [18, 19].

### C. Transfer Learning Theory

Existing theoretical studies in transfer learning can generally be divided into two primary categories. The first category aims to define and quantify the similarity or relatedness between source and target tasks. Numerous metrics have been proposed in this context, including the  $l_2$  distance [41], optimal transport cost [42], LEEP (Log Expected Empirical Prediction) [6], Wasserstein distance [19], OTCE (Optimal Transport-based Conditional Entropy) [43], LogME [44], NCE[45], GBC (Geometric-Based Correlation) [46], and maximal correlation-based measures [5]. For example, LEEP [6] provides a probabilistic framework for transferability estimation by comparing model predictions on the target task. Meanwhile, OTCE [43] leverages optimal transport theory to quantify transferability under distribution shifts. These measures provide principled ways to assess how well knowledge from a source task can potentially benefit a target task.

This work belongs to the second group, which is dedicated to developing theoretical measures that assess and bound the generalization error in transfer learning scenarios. Various generalization error measures have been proposed to guide the assignment of task or source weights, including mutual information [47],  $\chi^2$ -divergence [7], and  $\mathcal{H}$ -score [9]. Specifically, the  $\mathcal{H}$ -score facilitates the minimization of the bound of target generalization error by quantifying the importance of source tasks, thereby enabling an optimal weight assignment that prioritizes source representations with maximal discriminative information and minimal redundancy relative to the target domain.

Furthermore, a recently developed generalization measure based on K-L divergence [48] provides a rigorous foundation

for determining optimal transfer quantities. In this work, we demonstrate that such a measure offers a more direct alignment with the cross-entropy loss—a standard objective in machine learning—than previous metrics. Consequently, we extend this metric and framework to jointly optimize source weights and transfer quantities.

### III. PRELIMINARIES

#### A. K-L Divergence Based Measure

We will introduce a K-L divergence based measure as the generalization error measure.

**Definition 1** (The K-L divergence [49]). *The K-L divergence  $D(P\|Q)$  measures the difference between two probability distributions  $P(X)$  and  $Q(X)$  over the same probability space. It is defined as:*

$$D(P\|Q) = \sum_{x \in \mathcal{X}} p(x) \log \frac{p(x)}{q(x)}.$$

In this work, we use the expectation of K-L divergence between the true distribution of target task  $P_{X;\underline{\theta}_0}$  and the distribution  $P_{X;\hat{\underline{\theta}}}$  learned from training samples as the generalization error measure, i.e.,

$$\mathbb{E} \left[ D(P_{X;\underline{\theta}_0} \| P_{X;\hat{\underline{\theta}}}) \right]. \quad (1)$$

Compared to other measures, the K-L divergence exhibits a closer correspondence with the generalization error measured by the cross-entropy loss; we formally justify this relationship in Appendix D.

#### B. Problem Formulation

A multi-source transfer learning framework consists of a single target task  $\mathcal{T}$  and multiple source tasks  $\mathcal{S}_1, \dots, \mathcal{S}_K$  that provide auxiliary information for improving performance on the target. To generalize the analysis, we model  $\mathcal{T}$  as a parameter estimation problem governed by an underlying distribution  $P_{X;\underline{\theta}}$ . In typical settings such as supervised classification, this distribution corresponds to the joint probability model over input features  $Z$  and labels  $Y$ , where  $X = (Z, Y)$ , and  $\underline{\theta}$  denotes the parameter of interest. The goal is to accurately estimate the true value of  $\underline{\theta}$ , which corresponds to optimizing the network parameters of  $\mathcal{T}$  in deep learning. Furthermore, we assume that the source tasks and the target task follow the same parametric model and share the same input space  $\mathcal{X}$ . For notational clarity, we present only the case where  $\mathcal{X}$  is discrete, while the theoretical results extend straightforwardly to continuous domains. The target task  $\mathcal{T}$  has  $N_0$  independent and identically distributed (i.i.d.) training samples generated from the underlying distribution  $P_{X;\underline{\theta}_0}$ , where the parameter  $\underline{\theta}_0 \in \mathbb{R}^d$ , and we denote the training set as  $X^{N_0}$ . Similarly, the source task  $\mathcal{S}_i$  has a training set  $X^{N_i}$  with i.i.d.  $N_i$  training samples generated from distribution  $P_{X;\underline{\theta}_i}$ , where  $i \in [1, K]$ , and  $\underline{\theta}_i \in \mathbb{R}^d$ . During training, each sample is weighted in the gradient descent process according to the source weight of its corresponding task. Then, we formulate the training process as a parameter estimation problem and

give the form of the estimator.  $\hat{\underline{\theta}}$  is denoted as the MLE based on the  $N_0$  samples from  $\mathcal{T}$  and  $n_1, \dots, n_K$  samples from  $\mathcal{S}_1, \dots, \mathcal{S}_K$  with weights  $w_1, \dots, w_K$ , where  $n_i \in [0, N_i]$  and  $w_i \in [0, +\infty]$ , i.e.,

$$\hat{\underline{\theta}} = \arg \max_{\underline{\theta}} \sum_{x \in X^{N_0}} \log P_{X;\underline{\theta}}(x) + \sum_{i=1}^K \sum_{x \in X^{n_i}} w_i \log P_{X;\underline{\theta}}(x), \quad (2)$$

where we require  $w_i \geq 0$  because negative weights would subtract sample likelihoods, contradict the statistical meaning of MLE and turn the weighted log-likelihood into a non-concave and unbounded objective.

In this work, our goal is to derive the optimal transfer weight  $w_1^*, \dots, w_K^*$  and transfer quantities  $n_1^*, \dots, n_K^*$  of source tasks  $\mathcal{S}_1, \dots, \mathcal{S}_K$  to minimize the K-L based measure between the true distribution of target task  $P_{X;\underline{\theta}_0}$  and the distribution  $P_{X;\hat{\underline{\theta}}}$  learned from training samples, i.e.,

$$w_1^*, \dots, w_K^*, n_1^*, \dots, n_K^* = \arg \min_{w_1, \dots, w_K, n_1, \dots, n_K} \mathbb{E} \left[ D(P_{X;\underline{\theta}_0} \| P_{X;\hat{\underline{\theta}}}) \right]. \quad (3)$$

#### C. Asymptotic Normality of the MLE

When attempting to recover the true parameter vector  $\underline{\theta}^*$  from i.i.d observations generated according to the distribution  $P_{X;\underline{\theta}^*}$ , we let  $\mathcal{D}$  denote a collection of  $n$  such i.i.d. samples. The maximum likelihood estimator (MLE) is then defined as the maximizer of the empirical log-likelihood:

$$\hat{\underline{\theta}}_{\text{MLE}} = \arg \max_{\underline{\theta}} \frac{1}{n} \sum_{x \in \mathcal{D}} \log P_{X;\underline{\theta}}(x). \quad (4)$$

Provided that the underlying distribution satisfies the standard regularity assumptions, the MLE exhibits the well-known property of **asymptotic normality** [50]. Specifically, as the sample size increases, the distribution of the normalized estimation error converges in law to a multivariate Gaussian distribution:

$$\sqrt{n} (\hat{\underline{\theta}}_{\text{MLE}} - \underline{\theta}^*) \xrightarrow{d} \mathcal{N}(0, J(\underline{\theta}^*)^{-1}), \quad (5)$$

where the notation “ $-1$ ” indicates the matrix inverse, and  $J(\underline{\theta})$  denotes the Fisher information matrix [49]. The Fisher information matrix, which characterizes the amount of information carried by the distribution about the parameter, is defined as

$$J(\underline{\theta})^{d \times d} = \mathbb{E} \left[ \left( \frac{\partial}{\partial \underline{\theta}} \log P_{X;\underline{\theta}} \right) \left( \frac{\partial}{\partial \underline{\theta}} \log P_{X;\underline{\theta}} \right)^T \right]. \quad (6)$$

Intuitively, the Fisher information matrix quantifies the sensitivity of the likelihood function with respect to the parameter  $\underline{\theta}$ . A larger Fisher information implies that small changes in  $\underline{\theta}$  cause more pronounced variations in the log-likelihood, meaning the parameter is easier to estimate accurately from data. This notion is also closely related to the Cramér–Rao lower bound, which states that the covariance matrix of any unbiased estimator cannot be smaller (in the positive semi-definite sense) than the inverse of the Fisher information. Therefore, the Fisher information directly characterizes the fundamental limit of parameter estimation accuracy.

#### IV. MAIN RESULT

In this section, for the optimization problem in (3), we will first present the theoretical result and the computation method for the optimal transfer quantity and the optimal source weight in the single-source setting in Section IV-A. In the following, we extend the analysis to the multi-source setting in Section IV-B. Moreover, We introduce practical algorithms derived from our theory for multi-source transfer learning and multi-task learning in Section IV-C.

##### A. Single-Source Transfer Learning

In this subsection, we first analyze the case where the parameter is one-dimensional in Theorem 2. We then extend the method to the high-dimensional setting in Proposition 3. Throughout this paper, we denote scalar-valued parameters by  $\theta$  and high-dimensional parameters by  $\underline{\theta}$ . In analyzing the target parameter estimation problem, directly computing the K-L measure is intractable in general. Therefore, we conduct our analysis primarily in the asymptotic regime, where the behavior of the estimator becomes more tractable. To begin with, we consider the transfer learning scenario where we have one target task  $\mathcal{T}$  with  $N_0$  training samples and one source task  $\mathcal{S}_1$  with  $N_1$  training samples. In this case, we aim to determine the optimal transfer quantity  $n_1^* \in [1, N_1]$  and the optimal transfer weight  $w_1^* \in [0, +\infty]$ . To facilitate our mathematical derivations, we assume  $N_0$  and  $N_1$  are asymptotically comparable, and the distance between the parameters of the target task and source task is sufficiently small (*i.e.*,  $|\theta_0 - \theta_1| = O(\frac{1}{\sqrt{N_0}})$ ). Considering the similarity of low-level features among tasks of the same type, this assumption is made without loss of generality [48, 51]. Furthermore, as demonstrated in subsequent analysis, our conclusions remain valid even in extreme cases where the distance between parameters is large.

**Theorem 2.** (proved in Appendix A) *In single-source setting with 1-dimensional models  $P_{X;\theta_0}$  and  $P_{X;\theta_1}$ , we assume that  $\theta_0, \theta_1 \in \mathbb{R}$  and  $|\theta_0 - \theta_1| = O(\frac{1}{\sqrt{N_0}})$ . Then, the K-L measure  $\mathbb{E}[D(P_{X;\theta_0} || P_{X;\hat{\theta}})]$  can be expressed as:*

$$\frac{1}{2} \left( \underbrace{\frac{N_0 + w_1^2 n_1}{(N_0 + w_1 n_1)^2}}_{\text{variance term}} + \underbrace{\frac{w_1^2 n_1^2}{(N_0 + w_1 n_1)^2} t}_{\text{bias term}} \right) + o\left(\frac{1}{N_0}\right), \quad (7)$$

where

$$t \triangleq J(\theta_0)(\theta_1 - \theta_0)^2. \quad (8)$$

For **optimal transfer quantity**, by minimizing the above expression, we obtain that maximizing the transfer quantity is optimal, *i.e.*,

$$n_1^* = N_1. \quad (9)$$

Moreover, the solution of **optimal transfer weight**  $w_1^*$  is

$$w_1^* = \frac{1}{1 + t N_1}. \quad (10)$$

We now present some observations regarding the optimal weight in (10). We observe that as the distance between  $\theta_0$

and  $\theta_1$  increases, the optimal weight decreases. This shows that the weighting strategy reduces the influence of sources with substantial discrepancies from the target. Moreover, as the quantity of source samples  $N_1$  increases, the optimal weight also decreases. This illustrates that the derived weight adaptively controls the trade-off between the target and source information, preventing the source from dominating even when it is abundant. In Fig. 1, we provide an intuitive explanation for the optimal  $w_1^*$ .

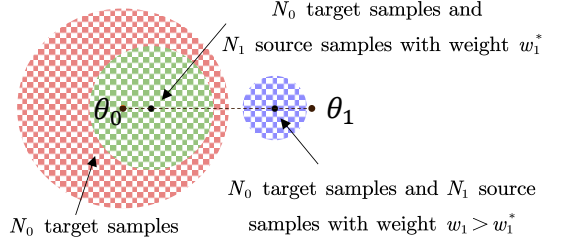


Fig. 1. The three circles represent the errors corresponding to transfer weight  $w_1 = 0$ ,  $w_1^*$ , and  $w_1 > w_1^*$ . The distance from each circle's center to  $\theta_0$  represents the bias of estimation, and the radius represents the variance. As the transfer weight of source increases, the bias term increases, while the variance term decreases for  $w_1 \in [0, 1]$  and increases for  $w_1 \in (1, +\infty)$ . The optimal  $w_1^*$  achieves the best trade-off between them.

In the following, we extend the result of the Theorem 2 to the high-dimensional setting.

**Proposition 3.** (proved in Appendix B) *In the single-source setting with  $d$ -dimensional models  $P_{X;\theta_0}$  and  $P_{X;\theta_1}$ , we assume that  $\underline{\theta}_0, \underline{\theta}_1 \in \mathbb{R}^d$  and  $\|\underline{\theta}_0 - \underline{\theta}_1\| = O(\frac{1}{\sqrt{N_0}})$ . Then, the K-L measure takes the following form:*

$$\frac{d}{2} \left( \frac{N_0 + w_1^2 n_1}{(N_0 + w_1 n_1)^2} + \frac{w_1^2 n_1^2}{(N_0 + w_1 n_1)^2} t \right) + o\left(\frac{1}{N_0}\right), \quad (11)$$

where

$$t \triangleq \frac{(\underline{\theta}_1 - \underline{\theta}_0)^\top J(\underline{\theta}_0)(\underline{\theta}_1 - \underline{\theta}_0)}{d}. \quad (12)$$

Here,  $t$  is a scalar ;  $J(\underline{\theta}_0) \in \mathbb{R}^{d \times d}$  denotes the Fisher information matrix evaluated at  $\underline{\theta}_0$ , and  $(\underline{\theta}_1 - \underline{\theta}_0) \in \mathbb{R}^d$  is the coordinate-wise difference between the two parameter vectors. Finally, the **optimal transfer quantity** is the same form as (9) and the **optimal transfer weight**  $w_1^*$  is the same form as (10).

Compared with Theorem 2, Proposition 3 retains an analogous structural form in its mathematical expression. This structural resemblance enables us to follow a conceptually similar analytical route to determine the corresponding optimal quantity of knowledge transfer. It is worth emphasizing that the appearance of the Fisher information matrix  $J$  in the  $t$ -term is a direct consequence of the theoretical derivation, rather than a modeling choice or an explicitly imposed mechanism. The resulting expression admits a clear interpretation: the Fisher information matrix implicitly induces a dimension-weighted aggregation over parameter directions, where the contribution of each direction is determined by the sensitivity of the likelihood. Parameter directions along which the likelihood is more sensitive to perturbations contribute more prominently

to the derived measure, while directions with lower sensitivity have a reduced influence. This interpretation clarifies that the role of  $J$  is inherent to the statistical structure of the estimation problem, rather than being introduced by design.

In addition, a closer inspection of Equation (11) reveals that the associated K-L measure exhibits a growth trend as the parameter dimensionality  $d$  increases. From a practical perspective, this scaling trend indicates that as models grow in complexity—characterized by increasingly large parameter spaces—the learning process becomes more intricate, thereby amplifying the challenge of achieving effective knowledge transfer. This observation is consistent with established findings in the literature [7], which indicate that increasing model complexity inherently exacerbates the difficulty of cross-task generalization.

**Remark 4** (Connection to Prior Work). *The expression in Theorem 2 and Proposition 3 coincides with the results obtained by [7]. The (23) can be transformed to*

$$\begin{aligned}\hat{\theta} &= \arg \max_{\theta} \frac{\sum_{x \in X^{N_0}} \log P_{X;\theta}(x) + \sum_{x \in X^{N_1}} w_1 \log P_{X;\theta}(x)}{N_0 + w_1 N_1}, \\ &= \arg \max_{\theta} \mathbb{E}_{\hat{P}_{\text{mix}}} [\log P_{X;\theta}(x)],\end{aligned}\quad (13)$$

where

$$\hat{P}_{\text{mix}} := \frac{N_0}{N_0 + w_1 N_1} \hat{P}(X_0^{N_0}) + \frac{w_1 N_1}{N_0 + w_1 N_1} \hat{P}(X_1^{N_1}). \quad (14)$$

Substituting the optimal weight (10) into (14), we have

$$\hat{P}_{\text{mix}} := \frac{t + \frac{1}{N_1}}{t + \frac{1}{N_0} + \frac{1}{N_1}} \hat{P}(X_0^N) + \frac{\frac{1}{N_0}}{t + \frac{1}{N_0} + \frac{1}{N_1}} \hat{P}(X_1^N). \quad (15)$$

This formulation exhibits a notable similarity to the conclusion presented in [7].

### B. Multi-Source Transfer Learning

In this subsection, we first present the expression of the K-L measure in the multi-source setting, as stated in Theorem 5. By minimizing this expression, we derive a method to compute the optimal source weights, and present practical algorithms for real-world multi-source transfer learning and multi-task learning scenarios in Algorithm 1 and Algorithm 2.

**Theorem 5.** (proved in Appendix C) *In the multi-source setting with  $d$ -dimensional models  $P_{X;\theta_0}$  for the target task and  $P_{X;\theta_i}$ ,  $i \in [1, K]$  for the source tasks, we assume that  $\theta_0, \theta_1 \dots \theta_K \in \mathbb{R}^d$  and  $\|\theta_0 - \theta_i\| = O(\frac{1}{\sqrt{N_0}})$ . Then, the K-L measure is given by*

$$\frac{d}{2} \left( \frac{N_0}{(N_0 + s)^2} + \frac{s^2}{(N_0 + s)^2} t \right) + o\left(\frac{1}{N_0}\right), \quad (16)$$

where we denote  $b_i = n_i w_i$ ,  $s = \sum_{i=1}^K b_i$ ,  $\alpha_i = \frac{b_i}{s}$ , and

$$t = \frac{\underline{\alpha}^T \left( \text{diag} \left( \frac{d}{n_1}, \dots, \frac{d}{n_K} \right) + \Theta^T J(\underline{\theta}_0) \Theta \right) \underline{\alpha}}{d}. \quad (17)$$

In (17),  $\underline{\alpha} = [\alpha_1, \dots, \alpha_K]^T$  is a  $K$ -dimensional vector, and

$$\Theta^{d \times K} = [\underline{\theta}_1 - \underline{\theta}_0, \dots, \underline{\theta}_K - \underline{\theta}_0]. \quad (18)$$

For **optimal transfer quantities**, by minimizing the (16), we obtain that maximizing the transfer quantities is optimal, i.e.,  $n_i^* = N_i$ . Moreover, we propose a numerical procedure to compute the **optimal source weights**, which will be elaborated in the paragraph following the proof.

We next present the method to compute the optimal value of  $w_i$  to minimize (16). The minimization problem is

$$(s^*, \underline{\alpha}^*) \leftarrow \arg \min_{(s, \underline{\alpha})} \frac{d}{2} \left( \frac{N_0}{(N_0 + s)^2} + \frac{s^2}{(N_0 + s)^2} t \right) + o\left(\frac{1}{N_0}\right). \quad (19)$$

We reformulate this optimization problem as a sequential optimization process, and explicitly formulate the constraints as follows.

$$(s^*, \underline{\alpha}^*) \leftarrow \arg \min_{s \in [0, +\infty]} \frac{d}{2} \left( \frac{N_0}{(N_0 + s)^2} + \frac{s^2}{(N_0 + s)^2} \cdot \right. \quad (20)$$

$$\left. \arg \min_{\underline{\alpha} \in \mathcal{A}} \frac{\underline{\alpha}^T \left( \text{diag} \left( \frac{d}{N_1}, \dots, \frac{d}{N_K} \right) + \Theta^T J(\underline{\theta}_0) \Theta \right) \underline{\alpha}}{d} \right), \quad (21)$$

where

$$\mathcal{A} = \left\{ \underline{\alpha} \left| \sum_{i=1}^K \alpha_i = 1, \alpha_i \geq 0, i = 1, \dots, K \right. \right\}. \quad (22)$$

This problem requires optimizing the objective function over two variables: a scalar variable  $s$  representing the total weighted transfer quantity, and a vector variable  $\underline{\alpha}$  representing the proportion of each source domain in  $s$ . First, we compute the optimal  $\underline{\alpha}'$  under the constraint  $\mathcal{A}$  to minimize  $t$ , and get the optimal  $\alpha_i^*$ ,  $i \in [1, K]$ , which is a  $K \times K$  non-negative quadratic programming problem with respect to  $\underline{\alpha}$

$$\underline{\alpha}^* = \arg \min_{\underline{\alpha} \in \mathcal{A}} \underline{\alpha}^T \frac{\left( \text{diag} \left( \frac{d}{N_1}, \dots, \frac{d}{N_K} \right) + \Theta^T J(\underline{\theta}_0) \Theta \right)}{d} \underline{\alpha}.$$

In the numerator of the quadratic coefficient matrix for this optimization problem, the first component is a diagonal matrix and is therefore strictly positive definite. The second component,  $\Theta^T J(\underline{\theta}_0) \Theta$ , is positive semi-definite because the Fisher information matrix  $J(\underline{\theta}_0)$  is itself positive semi-definite. By the closure property of positive semi-definite matrices under addition, the resulting quadratic coefficient matrix is also positive semi-definite. This property guarantees that the optimization problem admits at least one global optimal solution. By this procedure, we obtain  $t^*$  and  $\alpha^*$  that minimize  $t$ . Then we get the optimal value of  $s$ , which is always  $s^* = \frac{1}{t^*}$ . Finally, we use optimal  $s^*$  and  $\alpha_i^*$  to get the optimal weights by  $w_i^* = \frac{s^* \alpha_i^*}{N_i}$ .

The time complexity of this optimization method depends solely on the optimization of  $\alpha$ , which corresponds to a

$K \times K$  non-negative quadratic programming problem, whose complexity is  $\mathcal{O}(K^3)$ . In most standard transfer learning benchmarks, the number of available source domains is modest (typically  $K \leq 10$ ), rendering the  $\mathcal{O}(K^3)$  computational complexity manageable for real-world applications. For cases where the source domain set is substantially larger, one feasible strategy to preserve scalability is to perform a preliminary clustering or aggregation of domains with high similarity before executing our algorithm on the resulting reduced set.

**Remark 6** (Explanation of Using All Source Samples). *The finding that maximizing the transfer quantity is optimal is non-trivial and theoretically insightful. Conventional wisdom in transfer learning holds that excessive use of source data without controlling domain discrepancy can amplify bias and cause negative transfer [52]. This perspective has motivated many approaches that either down-weight or selectively discard source samples to mitigate distribution mismatch [11, 48]. On the other hand, some methods by default exploit all source data for joint training, often relying on heuristic weighting. Our framework provides a new theoretical perspective by jointly optimizing transfer quantity and source weights. Through asymptotic analysis, we prove that when weights are allowed to adjust, the optimal solution always employs all available source samples. The key insight is that enlarging the effective sample size strictly reduces variance, while the weighting mechanism simultaneously suppresses the bias introduced by heterogeneous domains. This dual effect reconciles the seemingly conflicting intuitions in the literature: discarding data may reduce bias but sacrifices variance reduction, whereas full data utilization achieves the best trade-off once proper weighting is in place. Consequently, our analysis offers a principled justification for exploiting all source data in multi-source transfer learning.*

### C. Practical Algorithms

In addition, we propose practical algorithms of UOWQ for multi-source transfer learning in Algorithm 1 and for multi-task learning in Algorithm 2. In the following, we focus on Algorithm 1 to illustrate the proposed approach, whose overall workflow is shown in Fig. 2. In UOWQ, when computing the optimal source weights based on Theorem 5, we use the parameters of pretrained source models to replace  $\theta_1, \dots, \theta_K$ . Considering that the source model can be trained using sufficient labeled data, it is reasonable to use the learned parameters as a good approximation of the true underlying parameters.

In contrast, the number of target data in transfer learning is often insufficient, so it is difficult to accurately estimate the true parameter  $\theta_0$  - the parameter of the target task model - using only the target data. Therefore, as shown in lines 5-12 of Algorithm 1, we adopt a **dynamic weight update strategy**. Specifically, in the first epoch, we train a  $\theta_0$  using only the target data. This  $\theta_0$  is then used, along with Theorem 5, to determine the optimal source weight of each source task. Finally, we continue training  $\theta_0$  with new weights, and this procedure is repeated in each subsequent epoch to iteratively

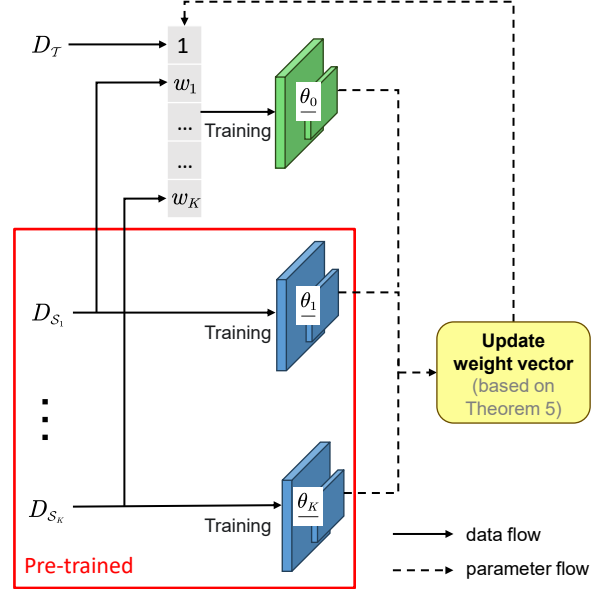


Fig. 2. **Overview of the UOWQ training pipeline:** At each iteration, the model parameters are optimized via gradient descent using target data together with weighted samples from each source task. The source weights are subsequently updated based on the current model parameters. This alternating optimization procedure establishes an iterative feedback loop that jointly updates the source weights and the target model.

update the weights. In summary, during the first epoch of the algorithm, a small set of target samples is utilized to initialize both the model parameters and the Fisher information matrix. In subsequent epochs, additional source samples are incorporated to refine this estimation, with the enlarged sample set enhancing the stability. In particular, the loss function  $\ell$  is the negative log-likelihood. Moreover, in line 9, we compute the matrix  $J$  using the widely adopted **empirical Fisher** approach in deep learning [53, 54].

## V. EXPERIMENTS

In this section, we evaluated the practical algorithms of UOWQ in real-world datasets. In particular, we evaluated Algorithm 1 in multi-source transfer learning setting and Algorithm 2 in multi-task learning setting.

### A. Experimental Settings

**Benchmark Datasets.** The **Office-Home** dataset [55] consists of four domains: **Art** (**Ar**, 2,427 samples), **Clipart** (**Cl**, 4,365 samples), **Product** (**Pr**, 4,439 samples), and **Real World** (**Rw**, 4,357 samples). Each domain contains images from the same 65 object categories, resulting in a total of 15,588 samples. The **DomainNet** dataset [56] comprises six distinct domains: **Clipart** (**Cl**, 48,841 samples), **Infograph** (**In**, 48,466 samples), **Painting** (**Pa**, 48,529 samples), **Quickdraw** (**Qd**, 48,755 samples), **Real** (**Re**, 120,906 samples), and **Sketch** (**Sk**, 49,044 samples). Each domain includes images from the same 345 object categories, yielding a total of 364,541 samples. Data examples of the two datasets are shown in Fig. 3. We treat the multi-class classification problem on each domain as an individual task.

---

**Algorithm 1** UOWQ for Multi-Source Transfer Learning
 

---

1: **Input:** Target data  $D_{\mathcal{T}} = \{(z_{\mathcal{T}}^j, y_{\mathcal{T}}^j)\}_{j=1}^{N_0}$ , source data  $\{D_{S_k} = \{(z_{S_k}^j, y_{S_k}^j)\}_{j=1}^{N_k}\}_{k=1}^K$ , model type  $f_{\underline{\theta}}$  and its parameters  $\underline{\theta}_0$  for target task and  $\{\underline{\theta}_k\}_{k=1}^K$  for source tasks, parameter dimension  $d$ , source weights  $\{w_k\}_{k=1}^K$   
 //  $z$  represents the feature and  $y$  represents the label

2: **Parameter:** Learning rate  $\eta$ .

3: **Initialize:** randomly initialize  $\underline{\theta}_0$ , use parameters of pre-trained source models to initialize  $\{\underline{\theta}_k\}_{k=1}^K$ , initialize weights  $\{w_k\}_{k=1}^K = 0$

4: **Output:** a well-trained  $\underline{\theta}_0$  for target task model  $f_{\underline{\theta}_0}$ .

5: **repeat**

6: 
$$\mathcal{L}_{train} \leftarrow \frac{\sum_{(z^j, y^j) \in D_{\mathcal{T}}} \ell(y^j, f_{\underline{\theta}_0}(z^j))}{|D_{\mathcal{T}} \cup \{D_{S_k}\}_{k=1}^K|}$$

$$+ \frac{\sum_{k=1}^K \sum_{(z^j, y^j) \in D_{S_k}} \ell(y^j, f_{\underline{\theta}_0}(z^j)) * w_k}{|D_{\mathcal{T}} \cup \{D_{S_k}\}_{k=1}^K|}$$

7:  $\underline{\theta}_0 \leftarrow \underline{\theta}_0 - \eta \nabla_{\underline{\theta}_0} \mathcal{L}_{train}$

8:  $\Theta \leftarrow [\underline{\theta}_1 - \underline{\theta}_0, \dots, \underline{\theta}_K - \underline{\theta}_0]^T$

9:  $J(\underline{\theta}_0) \leftarrow \frac{\sum_{(z^j, y^j) \in D_{\mathcal{T}}} \nabla_{\underline{\theta}_0} \ell(y^j, f_{\underline{\theta}_0}(z^j)) (\nabla_{\underline{\theta}_0} \ell(y^j, f_{\underline{\theta}_0}(z^j)))^T}{|D_{\mathcal{T}}|}$

10:  $(s^*, \underline{\alpha}^*) \leftarrow \arg \min_{(s, \underline{\alpha})} \frac{d}{2} \left( \frac{N_0}{(N_0+s)^2} + \frac{s^2}{(N_0+s)^2} t \right)$

11:  $w_k^* \leftarrow \frac{s^* \underline{\alpha}_k^*}{N_k}, k = 1, \dots, K$

12: **until**  $\underline{\theta}_0$  converges;

---

**Algorithm 2** UOWQ for Multi-Task Learning
 

---

1: **Input:** Datasets  $\{D_{S_k} = \{(z_{S_k}^j, y_{S_k}^j)\}_{j=1}^{N_k}\}_{k=1}^K$ , model type  $f_{\underline{\theta}}$ , parameters  $\{\underline{\theta}_k\}_{k=1}^K$ , parameter dimension  $d$ , weights  $\{w_k\}_{k=1}^K$

2: **Parameter:** Learning rate  $\eta$

3: **Initialize:** Randomly initialize  $\{\underline{\theta}_k\}_{k=1}^K$ , set weights  $w_{k'}^{(k)} = 0$  for all  $k \neq k'$

4: **Output:** well-trained parameters  $\{\underline{\theta}_k\}_{k=1}^K$

5: **repeat**

6: **for** each  $k = 1$  to  $K$  **do**

7: 
$$\mathcal{L}_{train}^{(k)} \leftarrow \frac{\sum_{(z^j, y^j) \in D_{S_k}} \ell(y^j, f_{\underline{\theta}_k}(z^j))}{|\{D_{S_k}\}_{k=1}^K|}$$

$$+ \frac{\sum_{k' \neq k} \sum_{(z^j, y^j) \in D_{S_{k'}}} \ell(y^j, f_{\underline{\theta}_k}(z^j)) * w_{k'}^{(k)}}{|\{D_{S_k}\}_{k=1}^K|}$$

8:  $\underline{\theta}_k \leftarrow \underline{\theta}_k - \eta \nabla_{\underline{\theta}_k} \mathcal{L}_{train}^{(k)}$

9:  $\Theta^{(k)} \leftarrow \left[ \underline{\theta}_1 - \underline{\theta}_k, \dots, \underline{\theta}_{k-1} - \underline{\theta}_k, \right.$ 

$$\left. \underline{\theta}_{k+1} - \underline{\theta}_k, \dots, \underline{\theta}_K - \underline{\theta}_k \right]$$

$$\sum_{(z^j, y^j) \in D_{S_k}} \nabla_{\underline{\theta}_k} \ell(y^j, f_{\underline{\theta}_k}(z^j)) (\nabla_{\underline{\theta}_k} \ell(y^j, f_{\underline{\theta}_k}(z^j)))^T$$

10:  $J^{(k)} \leftarrow \frac{|\{D_{S_k}\}_{k=1}^K|}{|D_{S_k}|}$

11:  $(s_k^*, \underline{\alpha}^{*(k)}) \leftarrow \arg \min_{(s, \underline{\alpha})} \frac{d}{2} \left( \frac{N_k}{(N_k+s)^2} + \frac{s^2}{(N_k+s)^2} t \right)$

12:  $w_{k'}^{(k)} \leftarrow \frac{s_k^* \underline{\alpha}_{k'}^{*(k)}}{N_{k'}}, \quad \forall k' \neq k$

13: **end for**

14: **until** all  $\underline{\theta}_k$  converge

---

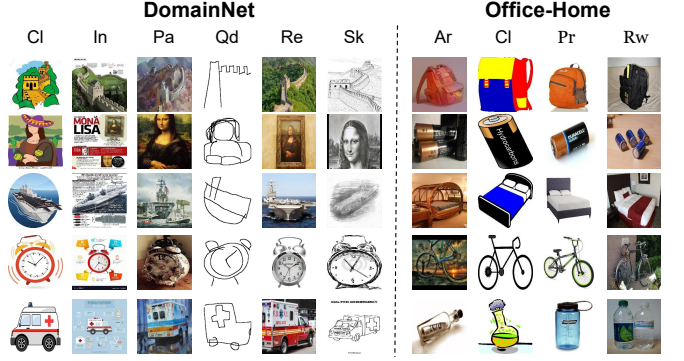


Fig. 3. **Overview of the Datasets:** Examples from the cross-domain datasets DomainNet and OfficeHome, where images from different domains exhibit distinct visual styles or are captured using different devices.

In the multi-source transfer learning setting, our goal is to transfer useful knowledge from multiple source domains to a specific target domain. In particular, our evaluation is performed in the 10-shot learning setting, where only 10 labeled samples per class are available in the target domain.

In multi-task learning setting, every task is simultaneously a target task to be learned and a source task from which knowledge is transferred to other tasks. Specifically, our approach iteratively selects one task as the target while treating others as sources, and derives weights through our theory. For each task, we construct its training set by combining all samples from the target domain with the weighted samples from the remaining domains, where the weights are again computed by UOWQ. All domain-specific tasks are then jointly optimized in a unified multi-task learning framework.

**Implementation Details.** Experiments are conducted on NVIDIA A800 GPU. To ensure fair comparison with prior work, different configurations are adopted for two scenarios. For the multi-source transfer learning setting, we adopt ViT-Small [57] pre-trained on ImageNet-21k [58] as the backbone and Adam optimizer [59] with a learning rate of  $10^{-5}$ . We allocate 20% of the dataset as the test set and report the best accuracy within 5 epochs of early stopping. For the multi-task learning setting, we use ResNet-18 [60] pre-trained on ImageNet-1k [61] as the backbone and Adam optimizer with a learning rate of  $10^{-4}$ . The dataset is randomly divided into 60% for training, 20% for validation, and 20% for testing.

### B. Experimental Design and Model Adaptation

**Baselines.** We compare our method with several SOTA methods in both settings.

For the multi-source transfer learning setting, we follow a unified evaluation setup for all methods. The baselines include: 1) Model-Weighting Based Few-Shot Methods: H-ensemble [9], MCW [5]. 2) Sample-Based Few-Shot Methods: MADA [18], WADN [19]. 3) Source Ablation Studies: Target-Only, Single-Source-Avg/Single-Source-Best (average/best single-source transfer results).

For the multi-task learning setting, we follow the same experimental setup as in [67] and compare with the baselines reported in their work. The baselines include: Equal Weighting (EW), MGDA-UB [29], GradNorm [27], PCGrad [64], CAGrad [31], RGW [65], MoCo [66], and MoDo [67].

TABLE II

MULTI-SOURCE TRANSFER PERFORMANCE ON DOMAINNET AND OFFICE-HOME. THE ARROWS INDICATE TRANSFERRING FROM THE REST TASKS. THE HIGHEST/SECOND-HIGHEST ACCURACY IS MARKED IN BOLD/UNDERSCORE FORM RESPECTIVELY.

Method	Backbone	DomainNet							Office-Home				
		→C	→I	→P	→Q	→R	→S	Avg	→Ar	→Cl	→Pr	→Rw	Avg
<b>Unsupervised-all-shots</b>													
MSFDA[62]	ResNet50	66.5	21.6	56.7	20.4	70.5	54.4	48.4	75.6	62.8	84.8	85.3	77.1
DATE[8]	ResNet50	-	-	-	-	-	-	-	75.2	60.9	<u>85.2</u>	84.0	76.3
M3SDA[63]	ResNet101	57.2	24.2	51.6	5.2	61.6	49.6	41.5	-	-	-	-	-
<b>Supervised-10-shots</b>													
<i>Few-Shot Methods:</i>													
H-ensemble[9]	ViT-S	53.4	21.3	54.4	19.0	70.4	44.0	43.8	71.8	47.5	77.6	79.1	69.0
MADA[18]	ViT-S	51.0	12.8	60.3	15.0	<b>81.4</b>	22.7	40.5	<u>78.4</u>	58.3	82.3	85.2	76.1
MCW[5]	ViT-S	54.9	21.0	53.6	20.4	70.8	42.4	43.9	68.9	48.0	77.4	<u>86.0</u>	70.1
WADN[19]	ViT-S	68.0	29.7	59.1	16.8	<u>74.2</u>	55.1	50.5	60.3	39.7	66.2	68.7	58.7
<i>Source-Ablation Methods:</i>													
Target-Only	ViT-S	14.2	3.3	23.2	7.2	41.4	10.6	16.7	40.0	33.3	54.9	52.6	45.2
Single-Source-Avg	ViT-S	50.4	22.1	44.9	24.7	58.8	42.5	40.6	65.2	53.3	74.4	72.7	66.4
Single-Source-Best	ViT-S	60.2	28.0	55.4	28.4	66.0	49.7	48.0	72.9	60.9	80.7	74.8	72.3
AllSources $\cup$ Target	ViT-S	71.7	32.4	60.0	31.4	71.7	58.5	54.3	77.0	62.3	84.9	84.5	77.2
OTQMS	ViT-S	<u>72.8</u>	<u>33.8</u>	<u>61.2</u>	<u>33.8</u>	73.2	<u>59.8</u>	<u>55.8</u>	78.1	<u>64.5</u>	<u>85.2</u>	84.9	<u>78.2</u>
UOWQ	ViT-S	<b>74.5</b>	<b>35.2</b>	<b>61.8</b>	<b>36.8</b>	73.3	<b>60.9</b>	<b>57.1</b>	<b>78.7</b>	<b>65.1</b>	<b>86.9</b>	<b>87.6</b>	<b>79.6</b>

TABLE III

MULTI-TASK LEARNING PERFORMANCE ON DOMAINNET AND OFFICE-HOME. EACH COLUMN INDICATES THE TARGET DOMAIN USED FOR EVALUATION. THE HIGHEST AND SECOND-HIGHEST ACCURACY ARE MARKED IN **BOLD** AND UNDERLINE, RESPECTIVELY.

Method	DomainNet							Office-Home				
	C	I	P	Q	R	S	Avg	Ar	Cl	Pr	Rw	Avg
EW	67.3	22.7	56.1	35.1	69.3	55.9	51.1	63.0	76.5	88.5	77.7	76.4
MGDA-UB[29]	69.0	22.4	<b>56.1</b>	31.7	69.7	55.9	50.8	64.3	75.3	89.7	79.3	77.2
GradNorm[27]	67.1	22.5	56.1	35.7	69.3	55.8	51.1	65.5	75.3	88.7	78.9	77.1
PCGrad[64]	67.8	22.7	<b>56.0</b>	34.7	69.2	56.1	51.1	63.9	76.0	88.9	78.3	76.8
CAGrad[31]	68.4	22.7	55.7	32.1	69.8	55.6	50.7	63.8	75.9	89.1	78.3	76.8
RGW[65]	67.1	21.9	55.2	33.9	68.6	55.6	50.4	65.1	78.7	88.7	79.9	78.1
MoCo[66]	60.3	19.0	46.6	39.9	57.9	50.7	45.7	64.1	<b>79.8</b>	89.6	79.6	78.3
MoDo[67]	67.9	22.0	55.4	36.0	69.4	56.3	51.2	66.2	78.2	<b>89.8</b>	80.3	78.7
UOWQ	<b>68.2</b>	<b>22.7</b>	<b>56.5</b>	<b>37.2</b>	<b>70.0</b>	<b>57.2</b>	<b>51.9</b>	<b>69.3</b>	77.3	89.5	<b>80.4</b>	<b>79.1</b>

TABLE IV

MULTI-TASK LEARNING PERFORMANCE ON DOMAINNET AND OFFICE-HOME. EACH COLUMN INDICATES THE TARGET DOMAIN USED FOR EVALUATION. THE HIGHEST AND SECOND-HIGHEST ACCURACY ARE MARKED IN **BOLD** AND UNDERLINE, RESPECTIVELY.

Method	DomainNet							Office-Home				
	C	I	P	Q	R	S	Avg	Ar	Cl	Pr	Rw	Avg
EW	67.3	<b>22.7</b>	<u>56.1</u>	35.1	69.3	55.9	51.1	63.0	76.5	88.5	77.7	76.4
MGDA-UB[29]	<b>69.0</b>	22.4	<u>56.1</u>	31.7	69.7	55.9	50.8	64.3	75.3	<u>89.7</u>	79.3	77.2
GradNorm[27]	67.1	<u>22.5</u>	<u>56.1</u>	35.7	69.3	55.8	51.1	65.5	75.3	88.7	78.9	77.1
PCGrad[64]	67.8	<b>22.7</b>	56.0	34.7	69.2	56.1	51.1	63.9	76.0	88.9	78.3	76.8
CAGrad[31]	68.4	<b>22.7</b>	55.7	32.1	<u>69.8</u>	55.6	50.7	63.8	75.9	89.1	78.3	76.8
RGW[65]	67.1	21.9	55.2	33.9	68.6	55.6	50.4	65.1	<u>78.7</u>	88.7	79.9	78.1
MoCo[66]	60.3	19.0	46.6	<b>39.9</b>	57.9	50.7	45.7	64.1	<b>79.8</b>	89.6	79.6	78.3
MoDo[67]	67.9	22.0	55.4	36.0	69.4	<u>56.3</u>	<u>51.2</u>	<u>66.2</u>	78.2	<b>89.8</b>	<u>80.3</u>	78.7
UOWQ	68.2	<b>22.7</b>	<b>56.5</b>	<u>37.2</u>	<b>70.0</b>	<b>57.2</b>	<b>51.9</b>	<b>69.3</b>	77.3	89.5	<b>80.4</b>	<b>79.1</b>

### C. Few-Shot Multi-Source Transfer Performance

We evaluated our method, UOWQ, against the baseline methods using the *Office-Home* and the *DomainNet* datasets. The quantitative results for the multi-source transfer learning setting are summarized in Table II. We make the following observations:

**Overall Performance.** In general, compared to the other baselines, UOWQ achieves the best performance. Specifically, in the multi-source transfer learning setting, UOWQ outperforms the state-of-the-art (OTQMS) by an average of 1.3% on *DomainNet* and 1.4% on *Office-Home*.

**Sample Weighting vs. Model Weighting.** In the multi-source transfer learning setting, methods based on sample weighting consistently exhibit stronger performance than those relying on model-level aggregation. Specifically, approaches that directly optimize a mixture of source and target samples—such as WADN, MADA, OTQMS, and UOWQ—tend to outperform model-weighting techniques like H-ensemble and MCW, which combine predictions or parameters from multiple pretrained models. A plausible explanation is that sample-weighting strategies allow the target model to interact directly with source data during training, enabling more flexible adaptation to target-specific distributions, whereas model-weighting methods are constrained by fixed source representations. Among sample-weighting approaches, UOWQ further improves upon existing baselines by jointly optimizing both the amount of transferred data and the corresponding weights, whereas OTQMS focuses on optimizing transfer quantities and WADN primarily adjusts weighting coefficients.

**Effectiveness of Limited Supervision.** We further compare supervised and unsupervised multi-source transfer learning approaches under otherwise identical settings. As shown in Table II, even when unsupervised methods such as MSFDA and M3SDA leverage all available target samples—up to  $1.3 \times 10^5$  instances in the *Real* domain of *DomainNet*—their performance remains inferior to supervised methods that utilize only a small number of labeled target samples (3450 in total). This comparison suggests that a modest amount of target supervision can provide substantially more informative guidance than large quantities of unlabeled data, underscoring the practical value of few-shot supervision in multi-source transfer learning.

**Gains over Strong Baselines in Challenging Domains.** Beyond average accuracy improvements, UOWQ consistently outperforms strong baselines in the most challenging domains. For example, in the experiments of *DomainNet* dataset, UOWQ improves over the previous best results in the *Quickdraw* target domain by 3.0% absolute accuracy (36.8% vs. 33.8%) and in the *Painting* target domain by 1.4% (35.2% vs. 33.8%). These gains in visually and semantically divergent domains demonstrate that UOWQ’s sample-weighting strategy is particularly effective in mitigating domain shift.

### D. Multi-Task Learning Performance

The results for the multi-task learning setting are summarized in Table IV. We make the following observations.

**Overall Performance Superiority.** Across both benchmarks, UOWQ achieves the best overall average performance. On *DomainNet*, it obtains the highest mean accuracy of 51.9%, improving upon the strongest baseline MoDo (51.2%) by 0.7 percentage points. Similarly, on *Office-Home*, UOWQ achieves the best average accuracy of 79.1%, surpassing MoDo (78.7%) and MoCo (78.3%) by 0.4 and 0.8 percentage points, respectively.

**Consistent and Balanced Multi-Task Performance.** Across the ten target domains from the two benchmarks, UOWQ achieves performance improvements on eight domains compared with the strongest competing methods, demonstrating broad effectiveness across heterogeneous tasks. In particular, the gains are consistent on *DomainNet*, where UOWQ outperforms all baselines across all six target domains (C, I, P, Q, R, and S), indicating that the improvements are not driven by a small subset of tasks. On *Office-Home*, while the improvements are more selective, UOWQ still attains the best overall average accuracy and achieves clear gains on two of the four target domains (Ar and Rw), while remaining competitive on the others. Importantly, improvements on more challenging domains do not come at the expense of degraded performance on easier ones, suggesting effective mitigation of negative task interference. Overall, these results highlight the ability of the proposed method to balance shared representation learning with task-specific optimization in multi-task settings.

**Theoretical Consistency.** Our theoretical analysis provides a clear explanation for the empirical observations in Table IV. Specifically, Theorems 5 shows that using the theoretically derived task weights leads to more balanced contributions from different tasks during multi-task optimization. This balanced weighting reduces the risk of over-emphasizing a single task and helps alleviate negative transfer caused by task mismatch. Empirically, this theoretical prediction is reflected in the experimental results: UOWQ achieves stable performance improvements across multiple target domains without exhibiting noticeable performance trade-offs. Consequently, the results on *DomainNet* and *Office-Home* provide empirical support for the effectiveness of the proposed weighting theory in multi-task learning settings.

### E. Weight Visualization

To analyze the domain preference learned by UOWQ, we visualize the coefficients  $\alpha$  obtained from the quadratic optimization problem together with the base weights  $w$  in Fig. 4, where each row corresponds to a target domain and each column corresponds to a source domain. The visualizations reveal clear and consistent patterns across both benchmarks. On *DomainNet*, when *Art*, *Clipart*, and *Product* are treated as target domains, the real-world domain consistently receives the largest  $\alpha$  coefficients. A similar trend is observed on *Office-Home* for *Art* and *Clipart* targets. Overall, these results indicate that the quadratic optimization naturally allocates higher transfer coefficients to more transferable source domains, consistent with prior empirical observations in [68].

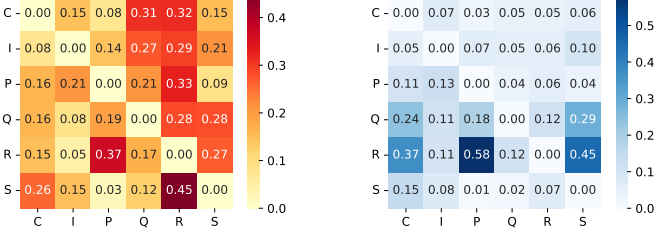
(a) DomainNet:  $\alpha$  weights(b) DomainNet:  $w$  weights(c) Office-Home:  $\alpha$  weights(d) Office-Home:  $w$  weights

Fig. 4. Domain preference visualization on DomainNet and Office-Home.

#### F. Robustness under Different Shot Settings

We further investigate the robustness of UOWQ with respect to the availability of target samples by gradually increasing the number of shots per class from 5 to 100. Fig. 5 reports the results on the Office-Home dataset across all four target domains (Ar, Cl, Pr, and Rw), in comparison with Target-Only and AllSources  $\cup$  Target. Across all domains, UOWQ maintains consistently competitive accuracy throughout the entire range of shot settings, showing neither performance collapse in low-shot regimes nor saturation-induced degradation as more target samples are introduced. In contrast to methods that rely heavily on either source aggregation or target-only supervision, UOWQ exhibits stable and monotonic performance trends as the number of shots increases. These observations indicate that the proposed approach adapts smoothly to different data regimes and remains robust under varying levels of target supervision.

#### G. Static vs. Dynamic Weighting.

Table V further examines the effect of dynamically updating source weights during training. Compared with the static variant, which fixes the weights computed at initialization, the dynamic strategy consistently achieves higher accuracy across all Office-Home target domains. The performance gap is particularly pronounced on more challenging domains such as Clipart and Product, indicating that continuously adapting the weights to the evolving target model is beneficial. These results suggest that dynamic re-optimization enables the transfer strategy to better track changes in the target representation, thereby suppressing suboptimal or outdated source contributions and improving overall robustness under limited target supervision.

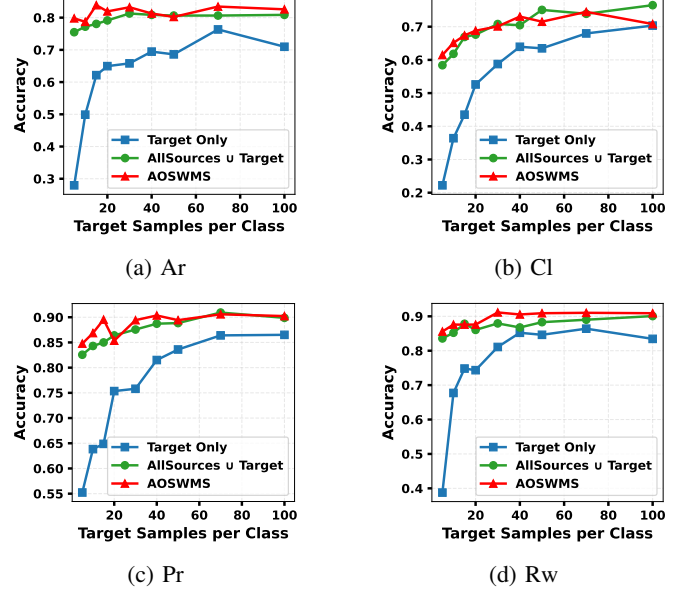


Fig. 5. Performance comparison on the Office-Home dataset under varying target shot settings.

TABLE V  
COMPARISON BETWEEN STATIC AND DYNAMIC WEIGHTING STRATEGIES  
UNDER THE 10-SHOT SETTING ON THE OFFICE-HOME DATASET.

Method	Backbone	Office-Home				
		$\rightarrow$ Ar	$\rightarrow$ Cl	$\rightarrow$ Pr	$\rightarrow$ Rw	Avg
<b>Supervised-10-shots:</b>						
Static	ViT-S	74.8	63.1	81.6	83.2	75.7
Dynamic	ViT-S	<b>78.7</b>	<b>65.1</b>	<b>86.9</b>	<b>87.6</b>	<b>79.6</b>

#### H. Computational Efficiency.

We further compare the computational cost of different methods on the DomainNet benchmark, and report the wall-clock training time in Table VI. Compared with MADA, which requires substantially longer training time across all target domains, both AllSources  $\cup$  Target and UOWQ exhibit significantly improved efficiency. Notably, UOWQ achieves comparable training time to AllSources  $\cup$  Target, with only a marginal overhead introduced by the additional optimization procedure. Across all domains, the average training time of UOWQ (10:00:32) remains close to that of AllSources  $\cup$  Target (09:50:10), and is substantially lower than MADA (17:07:55). These results indicate that the proposed method introduces minimal computational overhead while providing consistent performance gains, demonstrating a favorable trade-off between effectiveness and efficiency.

TABLE VI  
TRAINING TIME COMPARISON ON THE DOMAINNET DATASET ACROSS  
DIFFERENT TARGET DOMAINS.

Method	Backbone	DomainNet						
		$\rightarrow$ C	$\rightarrow$ I	$\rightarrow$ P	$\rightarrow$ Q	$\rightarrow$ R	$\rightarrow$ S	
MADA	ViT-S	15:57:00	20:01:00	17:23:30	24:07:30	11:15:00	14:03:30	17:07:55
AllSources $\cup$ Target	ViT-S	10:34:30	10:40:00	10:11:00	08:35:00	08:37:30	10:23:00	09:50:10
UOWQ	ViT-S	10:40:54	10:50:00	10:19:50	08:48:18	08:52:36	10:31:38	10:00:32

### I. Compatibility to LoRA-Based Training

We further examine the compatibility of UOWQ with LoRA. Specifically, we apply UOWQ to multi-source transfer on the **Office-Home** dataset using the ViT-B backbone. Each domain is treated as a distinct source task, and LoRA modules with rank 8 are inserted into the projection layers of transformer blocks. As summarized in Table VII, UOWQ consistently improves accuracy over baselines, confirming that the proposed theoretical principles remain effective under LoRA-based adaptation.

TABLE VII

MULTI-SOURCE TRANSFER WITH LORA ON OFFICE-HOME. WE APPLY LORA ON ViT-B BACKBONE FOR PEFT.

Method	Backbone	Office-Home				
		→Ar	→Cl	→Pr	→Rw	Avg
<b>Supervised-10-shots Source-Ablation:</b>						
Target-Only	ViT-B	59.8	42.2	69.5	72.0	60.9
Single-Source-avg	ViT-B	72.2	59.9	82.6	81.0	73.9
Single-Source-best	ViT-B	74.4	61.8	84.9	81.9	75.8
AllSources ∪ Target	ViT-B	<u>81.1</u>	66.0	88.0	89.2	81.1
OTQMS	ViT-B	<b>81.5</b>	<b>68.0</b>	<u>89.2</u>	<b>90.3</b>	<u>82.3</u>
UOWQ	ViT-B	<b>81.5</b>	<b>67.6</b>	<b>90.1</b>	<u>90.2</u>	<b>82.4</b>

### VI. CONCLUSION

In this work, we propose UOWQ, a theoretical framework for the unified optimization of source weights and transfer quantities in multi-source transfer learning. By formulating the training process as a parameter estimation problem and conducting an asymptotic analysis of a Kullback–Leibler-based generalization error measure, we derived a principled method for computing the optimal source weights and transfer quantities. A notable theoretical insight is that, once the weights are jointly optimized, the optimal solution always utilizes all source samples, while the adaptive weighting mechanism effectively suppresses the bias introduced by heterogeneous domains.

Building on these theoretical results, we further developed a practical algorithm that assigns sample-level weights and updates them dynamically during training. This design enables the framework to adapt to evolving model parameters and supports both multi-source transfer learning and multi-task learning scenarios.

Extensive experiments on real-world datasets demonstrate that UOWQ consistently improves performance over state-of-the-art baselines, particularly in few-shot and cross-domain settings. These results validate both the theoretical foundations and the practical advantages of our approach.

### REFERENCES

- [1] Z. Zhu, K. Lin, A. K. Jain, and J. Zhou, “Transfer learning in deep reinforcement learning: A survey,” *IEEE Transactions on Pattern Analysis and Machine Intelligence*, vol. 45, no. 11, pp. 13 344–13 362, 2023.
- [2] S. Serte, A. Serener, and F. Al-Turjman, “Deep learning in medical imaging: A brief review,” *Transactions on Emerging Telecommunications Technologies*, vol. 33, no. 10, p. e4080, 2022.
- [3] J. Devlin, M.-W. Chang, K. Lee, and K. Toutanova, “Bert: Pre-training of deep bidirectional transformers for language understanding,” in *Proceedings of the 2019 conference of the North American chapter of the association for computational linguistics: human language technologies, volume 1 (long and short papers)*, 2019, pp. 4171–4186.
- [4] Z. Wang, Z. Dai, B. Póczos, and J. Carbonell, “Characterizing and avoiding negative transfer,” in *Proceedings of the IEEE/CVF conference on computer vision and pattern recognition*, 2019, pp. 11 293–11 302.
- [5] J. Lee, P. Sattigeri, and G. Wornell, “Learning new tricks from old dogs: Multi-source transfer learning from pre-trained networks,” *Advances in neural information processing systems*, vol. 32, 2019.
- [6] C. Nguyen, T. Hassner, M. Seeger, and C. Archambeau, “Leep: A new measure to evaluate transferability of learned representations,” *International Conference on Machine Learning (ICML)*, 2020.
- [7] X. Tong, X. Xu, S.-L. Huang, and L. Zheng, “A mathematical framework for quantifying transferability in multi-source transfer learning,” *Advances in Neural Information Processing Systems*, vol. 34, pp. 26 103–26 116, 2021.
- [8] Z. Han, Z. Zhang, F. Wang, R. He, W. Su, X. Xi, and Y. Yin, “Discriminability and transferability estimation: a bayesian source importance estimation approach for multi-source-free domain adaptation,” in *Proceedings of the AAAI conference on artificial intelligence*, vol. 37, no. 6, 2023, pp. 7811–7820.
- [9] Y. Wu, J. Wang, W. Wang, and Y. Li, “H-ensemble: An information theoretic approach to reliable few-shot multi-source-free transfer,” in *Proceedings of the AAAI Conference on Artificial Intelligence*, vol. 38, no. 14, 2024, pp. 15 970–15 978.
- [10] D. Li, Z. Zhang, L. Wang, and H. R. Zhang, “Scalable fine-tuning from multiple data sources: A first-order approximation approach,” *Findings of the Association for Computational Linguistics: EMNLP 2024*, 2024.
- [11] S. Jain, H. Salman, A. Khaddaj, E. Wong, S. M. Park, and A. Mądry, “A data-based perspective on transfer learning,” in *Proceedings of the IEEE/CVF Conference on Computer Vision and Pattern Recognition*, 2023, pp. 3613–3622.
- [12] Q. Zhang, C. Chu, H. Fu, T. Peng, and S. Huang, “Asymptotic analysis for optimal source weights in multi-source transfer learning,” in *Proceedings of the APWD-SIT 2025*, 2025.
- [13] B. Liu, Y. Wei, Y. Zhang, and Q. Yang, “Task weighting in multi-task learning via gradient balancing,” *NeurIPS*, 2021.
- [14] X. Wang, J. Li, L. Jin, J. Pang, and D. Luo, “Multi-source domain adaptation with mixture of experts,” *ECCV*, 2020.
- [15] W. Zhou, H. Wen, and Y. Zhang, “Deep multi-source transfer learning for cross-domain recommendations,” *IEEE TKDE*, 2021.

[16] F. Zhuang, Z. Qi, K. Duan, D. Xi, Y. Zhu, H. Zhu, H. Xiong, and Q. He, “A comprehensive survey on transfer learning,” *Proceedings of the IEEE*, vol. 109, no. 1, pp. 43–76, 2020.

[17] L. Wan, R. Liu, L. Sun, H. Nie, and X. Wang, “Uav swarm based radar signal sorting via multi-source data fusion: A deep transfer learning framework,” *Information Fusion*, vol. 78, pp. 90–101, 2022.

[18] W. Zhang, Z. Lv, H. Zhou, J.-W. Liu, J. Li, M. Li, Y. Li, D. Zhang, Y. Zhuang, and S. Tang, “Revisiting the domain shift and sample uncertainty in multi-source active domain transfer,” in *Proceedings of the IEEE/CVF Conference on Computer Vision and Pattern Recognition*, 2024, pp. 16 751–16 761.

[19] C. Shui, Z. Li, J. Li, C. Gagné, C. X. Ling, and B. Wang, “Aggregating from multiple target-shifted sources,” in *International Conference on Machine Learning*. PMLR, 2021, pp. 9638–9648.

[20] Y. Li, L. Yuan, Y. Chen, P. Wang, and N. Vasconcelos, “Dynamic transfer for multi-source domain adaptation,” in *Proceedings of the IEEE/CVF Conference on Computer Vision and Pattern Recognition*, 2021, pp. 10 998–11 007.

[21] S. Zhao, H. Chen, H. Huang, P. Xu, and G. Ding, “More is better: Deep domain adaptation with multiple sources,” *arXiv preprint arXiv:2405.00749*, 2024.

[22] K. Li, J. Lu, H. Zuo, and G. Zhang, “Multi-source contribution learning for domain adaptation,” *IEEE Transactions on Neural Networks and Learning Systems*, vol. 33, no. 10, pp. 5293–5307, 2021.

[23] S. Zhao, B. Li, P. Xu, X. Yue, G. Ding, and K. Keutzer, “Madan: Multi-source adversarial domain aggregation network for domain adaptation,” *International Journal of Computer Vision*, vol. 129, no. 8, pp. 2399–2424, 2021.

[24] H. Guo, R. Pasunuru, and M. Bansal, “Multi-source domain adaptation for text classification via distancenet-bandits,” in *Proceedings of the AAAI conference on artificial intelligence*, vol. 34, no. 05, 2020, pp. 7830–7838.

[25] R. Caruana, “Multitask learning,” *Machine learning*, vol. 28, no. 1, pp. 41–75, 1997.

[26] A. Kendall, Y. Gal, and R. Cipolla, “Multi-task learning using uncertainty to weigh losses for scene geometry and semantics,” in *Proceedings of the IEEE Conference on Computer Vision and Pattern Recognition (CVPR)*, 2018. [Online]. Available: <https://arxiv.org/abs/1705.07115>

[27] Z. Chen, V. Badrinarayanan, C.-Y. Lee, and A. Rabinovich, “Gradnorm: Gradient normalization for adaptive loss balancing in deep multitask networks,” in *International Conference on Machine Learning (ICML)*, 2018. [Online]. Available: <https://arxiv.org/abs/1711.02257>

[28] S. Liu, E. Johns, and A. J. Davison, “End-to-end multi-task learning with attention,” in *Proceedings of the IEEE Conference on Computer Vision and Pattern Recognition (CVPR)*, 2019. [Online]. Available: <https://arxiv.org/abs/1803.10704>

[29] O. Sener and V. Koltun, “Multi-task learning as multi-objective optimization,” in *Advances in Neural Information Processing Systems (NeurIPS)*, 2018. [Online]. Available: <https://arxiv.org/abs/1810.04650>

[30] X. Zheng, Y. Liu, Y. Hua, Y. Tian, and T. Zhang, “Libra: Balancing tasks for multi-task learning,” in *International Conference on Machine Learning (ICML)*, 2021. [Online]. Available: <https://arxiv.org/abs/2107.07018>

[31] B. Liu, X. Liu, X. Jin, P. Stone, and Q. Liu, “Conflict-averse gradient descent for multi-task learning,” in *Advances in Neural Information Processing Systems (NeurIPS)*, 2021. [Online]. Available: <https://arxiv.org/abs/2010.14030>

[32] Q. Sun, Y. Liu, T.-S. Chua, and B. Schiele, “Adaptive task sampling for meta-learning,” in *Advances in Neural Information Processing Systems (NeurIPS)*, 2020. [Online]. Available: <https://arxiv.org/abs/2006.15586>

[33] K.-K. Maninis, I. Radosavovic, and I. Kokkinos, “Rotograd: Gradient homogenization in multitask learning,” in *International Conference on Learning Representations (ICLR)*, 2022, notable Top 5% Paper. [Online]. Available: <https://arxiv.org/abs/2103.14010>

[34] Y. Du, J. Lin, and P. Zhou, “Game-theoretic optimization for multi-task learning,” in *Advances in Neural Information Processing Systems (NeurIPS)*, 2023. [Online]. Available: <https://arxiv.org/abs/2302.02842>

[35] T. Chen, Y. Sun, and W. Yin, “Flix: A simple and communication-efficient alternative to local methods in federated learning,” in *International Conference on Machine Learning (ICML)*, 2023. [Online]. Available: <https://arxiv.org/abs/2302.02842>

[36] E. Triantafillou, T. Zhu, V. Dumoulin, P. Lamblin, U. Evci, K. Xu, R. Goroshin, C. Gelada, K. Swersky, P.-A. Manzagol *et al.*, “Meta-dataset: A dataset of datasets for learning to learn from few examples,” in *International Conference on Learning Representations (ICLR)*, 2020. [Online]. Available: <https://arxiv.org/abs/1903.03096>

[37] Y. Mansour, M. Mohri, and A. Rostamizadeh, “Domain adaptation with multiple sources,” *Advances in neural information processing systems*, vol. 21, 2008.

[38] M. Long, Y. Cao, J. Wang, and M. Jordan, “Learning transferable features with deep adaptation networks,” in *International conference on machine learning*. PMLR, 2015, pp. 97–105.

[39] H. Zhao, S. Zhang, G. Wu, J. M. Moura, J. P. Costeira, and G. J. Gordon, “Adversarial multiple source domain adaptation,” *Advances in neural information processing systems*, vol. 31, 2018.

[40] Y. Chen, W. Li, C. Sakaridis, D. Dai, and L. Van Gool, “Domain adaptive faster r-cnn for object detection in the wild,” in *Proceedings of the IEEE conference on computer vision and pattern recognition*, 2018, pp. 3339–3348.

[41] M. Long, J. Wang, G. Ding, J. Sun, and P. S. Yu, “Transfer joint matching for unsupervised domain adaptation,” in *Proceedings of the IEEE conference on computer vision and pattern recognition*, 2014, pp. 1410–1417.

[42] N. Courty, R. Flamary, D. Tuia, and A. Rakotomamonjy, “Optimal transport for domain adaptation,” *IEEE transactions on pattern analysis and machine intelligence*, vol. 39, no. 9, pp. 1853–1865, 2016.

[43] X. Chen, S. Wang, J. Wang, and Y. Huang, “Otce: Optimal transport for conditional entropy in transfer learning,” *NeurIPS*, 2022.

[44] K. You, Y. Liu, J. Wang, and M. Long, “Logme: Practical assessment of pre-trained models for transfer learning,” *International Conference on Machine Learning (ICML)*, 2021.

[45] C. Tan, F. Sun, T. Kong, W. Zhang, C. Yang, and C. Liu, “A survey on deep transfer learning,” *Neural Networks*, vol. 121, pp. 135–151, 2020.

[46] H. Liu, M. Long, J. Wang, and Y. Wang, “Geometric-based domain adaptation for transfer learning,” *AAAI Conference on Artificial Intelligence*, 2021.

[47] Y. Bu, S. Zou, and V. V. Veeravalli, “Tightening mutual information-based bounds on generalization error,” *IEEE Journal on Selected Areas in Information Theory*, vol. 1, no. 1, pp. 121–130, 2020.

[48] Q. Zhang, H. Fu, G. Huang, Y. Liang, C. Chu, T. Peng, Y. Wu, Q. Li, Y. Li, and S.-L. Huang, “A high-dimensional statistical method for optimizing transfer quantities in multi-source transfer learning,” in *The Thirty-ninth Annual Conference on Neural Information Processing Systems*, 2025. [Online]. Available: <https://openreview.net/forum?id=fsTj0BNxyH>

[49] T. M. Cover, *Elements of information theory*. John Wiley & Sons, 1999.

[50] A. W. Van der Vaart, *Asymptotic statistics*. Cambridge university press, 2000, vol. 3.

[51] M. Raghu, C. Zhang, J. Kleinberg, and S. Bengio, “Transfusion: Understanding transfer learning for medical imaging,” *Advances in neural information processing systems*, vol. 32, 2019.

[52] W. Zhang, L. Deng, L. Zhang, and D. Wu, “A survey on negative transfer,” *IEEE/CAA Journal of Automatica Sinica*, vol. 10, no. 2, pp. 305–329, 2022.

[53] J. Martens, “New insights and perspectives on the natural gradient method,” *Journal of Machine Learning Research*, vol. 21, no. 146, pp. 1–76, 2020.

[54] K. Osawa, S. Li, and T. Hoeffler, “Pipefisher: Efficient training of large language models using pipelining and fisher information matrices,” *Proceedings of Machine Learning and Systems*, vol. 5, pp. 708–727, 2023.

[55] H. Venkateswara, J. Eusebio, S. Chakraborty, and S. Panchanathan, “Deep hashing network for unsupervised domain adaptation,” in *Proceedings of the IEEE conference on computer vision and pattern recognition*, 2017, pp. 5018–5027.

[56] X. Peng, Q. Bai, X. Xia, Z. Huang, K. Saenko, and B. Wang, “Moment matching for multi-source domain adaptation,” in *Proceedings of the IEEE/CVF international conference on computer vision*, 2019, pp. 1406–1415.

[57] R. Wightman, “Pytorch image models,” <https://github.com/huggingface/pytorch-image-models>, 2019.

[58] J. Deng, W. Dong, R. Socher, L.-J. Li, K. Li, and L. Fei-Fei, “Imagenet: A large-scale hierarchical image database,” in *2009 IEEE conference on computer vision and pattern recognition*. Ieee, 2009, pp. 248–255.

[59] D. P. Kingma and J. Ba, “Adam: A method for stochastic optimization,” *arXiv preprint arXiv:1412.6980*, 2014.

[60] K. He, X. Zhang, S. Ren, and J. Sun, “Deep residual learning for image recognition,” in *Proceedings of the IEEE conference on computer vision and pattern recognition*, 2016, pp. 770–778.

[61] A. Krizhevsky, I. Sutskever, and G. E. Hinton, “Imagenet classification with deep convolutional neural networks,” *Advances in neural information processing systems*, vol. 25, 2012.

[62] M. Shen, Y. Bu, and G. W. Wornell, “On balancing bias and variance in unsupervised multi-source-free domain adaptation,” in *International Conference on Machine Learning*. PMLR, 2023, pp. 30976–30991.

[63] X. Peng, Q. Bai, X. Xia, Z. Huang, K. Saenko, and B. Wang, “Moment matching for multi-source domain adaptation,” in *Proceedings of the IEEE/CVF international conference on computer vision*, 2019, pp. 1406–1415.

[64] T. Yu, S. Kumar, A. Gupta, S. Levine, K. Hausman, and C. Finn, “Gradient surgery for multi-task learning,” in *International Conference on Learning Representations (ICLR)*, 2020. [Online]. Available: <https://arxiv.org/abs/2001.06782>

[65] B. Lin, F. Ye, Y. Zhang, and I. Tsang, “Reasonable effectiveness of random weighting: A litmus test for multi-task learning,” *Transactions on Machine Learning Research*.

[66] H. Fernando, H. Shen, M. Liu, S. Chaudhury, K. Murgesan, and T. Chen, “Mitigating gradient bias in multi-objective learning: A provably convergent stochastic approach,” 2023.

[67] L. Chen, H. Fernando, Y. Ying, and T. Chen, “Three-way trade-off in multi-objective learning: Optimization, generalization and conflict-avoidance,” *Advances in Neural Information Processing Systems*, vol. 36, pp. 70045–70093, 2023.

[68] J. Liang, D. Hu, and J. Feng, “Do we really need to access the source data? source hypothesis transfer for unsupervised domain adaptation,” in *International conference on machine learning*. PMLR, 2020, pp. 6028–6039.

APPENDIX A  
PROOF OF THEOREM 2

*Proof.* In this setting, the MLE and its expected definition are given as follows.

$$\hat{\theta} \triangleq \arg \max_{\theta} L_n(\theta), \quad (23)$$

$$E_{\hat{\theta}} \triangleq \arg \max_{\theta} L(\theta). \quad (24)$$

where

$$L_n(\theta) = \frac{\sum_{x \in X^{N_0}} \log P_{X;\theta}(x) + \sum_{x \in X^{n_1}} w_1 \log P_{X;\theta}(x)}{N_0 + w_1 n_1}, \quad (25)$$

$$L(\theta) = \frac{N_0 \mathbb{E}_{\theta_0} [\log P_{X;\theta}(x)] + w_1 n_1 \mathbb{E}_{\theta_1} [\log P_{X;\theta}(x)]}{N_0 + w_1 n_1}. \quad (26)$$

For  $E_{\hat{\theta}}$ , we have the following lemma to establish its relation to the  $\theta_0$  and  $\theta_1$ .

**Lemma 7.**  $E_{\hat{\theta}}$  is a weighted average of  $\theta_0$  and  $\theta_1$ , given by

$$E_{\hat{\theta}} = \frac{N_0 \theta_0 + w_1 n_1 \theta_1}{N_0 + w_1 n_1} + O\left(\frac{1}{N_0}\right). \quad (27)$$

*Proof.* We could equivalently transform (24) into

$$E_{\hat{\theta}} \triangleq \arg \min_{\theta} -L(\theta). \quad (28)$$

We then employ the Lagrangian method to solve this minimization problem. We treat  $P_{X;\theta}(x), \forall x \in \mathcal{X}$  as the variables with constraint

$$\sum_{x \in \mathcal{X}} P_{X;\theta}(x) = 1. \quad (29)$$

Then we can construct the corresponding Lagrangian function

$$\text{Lagrangian}(P, \lambda) = - \sum_{x \in \mathcal{X}} \left( \frac{N_0 P_{X;\theta_0}(x)}{N_0 + w_1 n_1} + \frac{w_1 n_1 P_{X;\theta_1}(x)}{N_0 + w_1 n_1} \right) \log P_{X;\theta}(x) + \lambda \left( \sum_{x \in \mathcal{X}} P_{X;\theta}(x) - 1 \right). \quad (30)$$

By jointly solving the first-order necessary conditions

$$\frac{\partial \text{Lagrangian}(P, \lambda)}{\partial P_{X;\theta}(x)} = 0, \forall x \in \mathcal{X} \quad (31)$$

$$\frac{\partial \text{Lagrangian}(P, \lambda)}{\partial \lambda} = 0, \quad (32)$$

we have

$$P_{X;E_{\hat{\theta}}}(x) = \frac{N_0 P_{X;\theta_0}(x) + w_1 n_1 P_{X;\theta_1}(x)}{N_0 + w_1 n_1}, \forall x \in \mathcal{X}. \quad (33)$$

By doing a Taylor Expansion of (33) around  $\theta_0$ , we can get

$$\begin{aligned} P_{X;\theta_0}(x) + \frac{\partial P_{X;\theta_0}(x)}{\partial \theta} (E_{\hat{\theta}} - \theta_0) + O(|E_{\hat{\theta}} - \theta_0|^2) \\ = \frac{N_0}{N_0 + w_1 n_1} P_{X;\theta_0}(x) + \frac{w_1 n_1}{N_0 + w_1 n_1} \left( P_{X;\theta_0}(x) + \frac{\partial P_{X;\theta_0}(x)}{\partial \theta} (\theta_1 - \theta_0) + O(|\theta_0 - \theta_1|^2) \right). \end{aligned} \quad (34)$$

From (34) we can get

$$E_{\hat{\theta}} = \frac{N_0 \theta_0 + w_1 n_1 \theta_1}{N_0 + w_1 n_1} + O(|\theta_0 - \theta_1|^2), \quad (35)$$

So we can get

$$E_{\hat{\theta}} = \frac{N_0 \theta_0 + w_1 n_1 \theta_1}{N_0 + w_1 n_1} + O\left(\frac{1}{N_0}\right). \quad (36)$$

□

Because  $\hat{\theta}$  is a maximizer of  $L_n(\hat{\theta})$ ,  $E_{\hat{\theta}}$  is a maximizer of  $L(\hat{\theta})$ , we can get

$$L'_n(\hat{\theta}) = 0 = L'_n(E_{\hat{\theta}}) + L''_n(E_{\hat{\theta}})(\hat{\theta} - E_{\hat{\theta}}), \quad (37)$$

$$\begin{aligned} L'(E_{\hat{\theta}}) = 0 = & \frac{N_0}{N_0 + w_1 n_1} \mathbb{E}_{\theta_0} \left[ \frac{\partial \log P_{X;E_{\hat{\theta}}}(x)}{\partial \theta} \right] \\ & + \frac{w_1 n_1}{N_0 + w_1 n_1} \mathbb{E}_{\theta_1} \left[ \frac{\partial \log P_{X;E_{\hat{\theta}}}(x)}{\partial \theta} \right]. \end{aligned} \quad (38)$$

By transforming (37), we have

$$\sqrt{N_0 + w_1 n_1} (\hat{\theta} - E_{\hat{\theta}}) = - \frac{\sqrt{N_0 + w_1 n_1} L'_n(E_{\hat{\theta}})}{L''_n(E_{\hat{\theta}})}. \quad (39)$$

Combining with (38), we can get

$$\begin{aligned} & \sqrt{N_0 + w_1 n_1} L'_n(E_{\hat{\theta}}) \\ &= \sqrt{N_0 + w_1 n_1} (L'_n(E_{\hat{\theta}}) - L'(E_{\hat{\theta}})) \\ &= \sqrt{\frac{N_0}{N_0 + w_1 n_1}} \left( \sqrt{\frac{1}{N_0}} \sum_{x \in X^{N_0}} \frac{\partial \log P_{X;E_{\hat{\theta}}}(x)}{\partial \theta} \right. \\ & \quad \left. - \sqrt{N_0} \mathbb{E}_{\theta_0} \left[ \frac{\partial \log P_{X;E_{\hat{\theta}}}(x)}{\partial \theta} \right] \right) \\ &+ \sqrt{\frac{w_1 n_1}{N_0 + w_1 n_1}} \left( \sqrt{\frac{1}{w_1 n_1}} \sum_{x \in X^{n_1}} w_1 \frac{\partial \log P_{X;E_{\hat{\theta}}}(x)}{\partial \theta} \right. \\ & \quad \left. - \sqrt{w_1 n_1} \mathbb{E}_{\theta_1} \left[ \frac{\partial \log P_{X;E_{\hat{\theta}}}(x)}{\partial \theta} \right] \right). \end{aligned} \quad (40)$$

Applying the Central Limit Theorem to (40), we can get

$$\sqrt{N_0 + w_1 n_1} L'_n(E_{\hat{\theta}}) \xrightarrow{a.s.} \quad (41)$$

$$\begin{aligned} & \mathcal{N} \left( 0, \frac{N_0}{N_0 + w_1 n_1} \left( \mathbb{E}_{\theta_0} \left[ \left( \frac{\partial \log P_{X;E_{\hat{\theta}}}(x)}{\partial \theta} \right)^2 \right] \right. \right. \\ & \quad \left. \left. - \mathbb{E}_{\theta_0} \left[ \left( \frac{\partial \log P_{X;E_{\hat{\theta}}}(x)}{\partial \theta} \right) \right]^2 \right] \right) + \\ & \quad \frac{w_1 n_1}{N_0 + w_1 n_1} \left( \mathbb{E}_{\theta_1} \left[ \left( \frac{\partial \log P_{X;E_{\hat{\theta}}}(x)}{\partial \theta} \right)^2 \right] \right. \\ & \quad \left. \left. - \mathbb{E}_{\theta_1} \left[ \left( \frac{\partial \log P_{X;E_{\hat{\theta}}}(x)}{\partial \theta} \right) \right]^2 \right] \right) \end{aligned} \quad (42)$$

By taking Taylor expansion of  $E_{\hat{\theta}}$  at  $\theta_0$ , we can get

$$\begin{aligned}
& \mathbb{E}_{\theta_0} \left[ \left( \frac{\partial \log P_{X;E_{\hat{\theta}}}(x)}{\partial \theta} \right)^2 \right] \\
&= \mathbb{E}_{\theta_0} \left[ \left( \frac{\partial \log P_{X;\theta_0}(x)}{\partial \theta} + \frac{\partial}{\partial \theta} \frac{\partial \log P_{X;\theta_0}(x)}{\partial \theta} (E_{\hat{\theta}} - \theta_0) \right. \right. \\
&\quad \left. \left. + O\left(\frac{1}{N_0}\right) \right)^2 \right] \\
&= J(\theta_0) + (E_{\hat{\theta}} - \theta_0) \mathbb{E}_{\theta_0} \left[ \frac{\partial \log P_{X;E_{\hat{\theta}}}(x)}{\partial \theta} \frac{\partial^2 \log P_{X;E_{\hat{\theta}}}(x)}{\partial \theta^2} \right] \\
&\quad + O\left(\frac{1}{N_0}\right) \\
&= J(\theta_0) + O\left(\frac{1}{\sqrt{N_0}}\right) \tag{43}
\end{aligned}$$

and

$$\begin{aligned}
& \mathbb{E}_{\theta_0} \left[ \left( \frac{\partial \log P_{X;E_{\hat{\theta}}}(x)}{\partial \theta} \right)^2 \right] \\
&= \mathbb{E}_{\theta_0} \left[ \left( \frac{\partial \log P_{X;\theta_0}(x)}{\partial \theta} + \frac{\partial}{\partial \theta} \frac{\partial \log P_{X;\theta_0}(x)}{\partial \theta} (E_{\hat{\theta}} - \theta_0) \right. \right. \\
&\quad \left. \left. + O\left(\frac{1}{N_0}\right) \right)^2 \right] \\
&= \mathbb{E}_{\theta_0} \left[ \left( \frac{\partial}{\partial \theta} \frac{\partial \log P_{X;\theta_0}(x)}{\partial \theta} (E_{\hat{\theta}} - \theta_0) + O\left(\frac{1}{N_0}\right) \right)^2 \right] \\
&= (E_{\hat{\theta}} - \theta_0)^2 \mathbb{E}_{\theta_0} \left[ \left( \frac{\partial}{\partial \theta} \frac{\partial \log P_{X;\theta_0}(x)}{\partial \theta} \right)^2 \right] + o\left(\frac{1}{N_0}\right) \\
&= O\left(\frac{1}{N_0}\right) \tag{44}
\end{aligned}$$

By combining (41), (43), and (44), we can get

$$\begin{aligned}
& \sqrt{N_0 + w_1 n_1} L'_n(E_{\hat{\theta}}) \xrightarrow{a.s.} \\
& \mathcal{N} \left( 0, \frac{N_0}{N_0 + w_1 n_1} J(\theta_0) + \frac{w_1^2 n_1}{N_0 + w_1 n_1} J(\theta_1) \right). \tag{45}
\end{aligned}$$

Moreover, we know  $L''_n(E_{\hat{\theta}}) \xrightarrow{P} -J(E_{\hat{\theta}})$ . Given that  $\theta_0, \theta_1$ , and  $E_{\hat{\theta}}$  are already assumed to be sufficiently close, we can use this, along with a Taylor expansion, to estimate the distance between their Fisher information matrices. We conclude that the discrepancy among  $J(\theta_0)$ ,  $J(\theta_1)$ , and  $J(E_{\hat{\theta}})$  is of the order

$$O\left(\frac{1}{\sqrt{N_0}}\right).$$

$$\begin{aligned}
J(\theta_1) &= \mathbb{E}_{\theta_1} \left[ \left( \frac{\partial}{\partial \theta} \log P_{X;\theta_1} \right)^2 \right] \\
&= \mathbb{E}_{\theta_1} \left[ \left( \frac{\partial}{\partial \theta} \log P_{X;\theta_0} + \frac{\partial^2 \log P_{X;\theta_0}}{\partial \theta^2} (\theta_1 - \theta_0) \right. \right. \\
&\quad \left. \left. + O\left(\frac{1}{N_0}\right) \right)^2 \right] \\
&= \mathbb{E}_{\theta_1} \left[ \left( \frac{\partial}{\partial \theta} \log P_{X;\theta_0} \right)^2 \right] + O\left(\frac{1}{\sqrt{N_0}}\right) \\
&= \sum_{x \in \mathcal{X}} P_{X;\theta_1}(x) \left( \frac{\partial}{\partial \theta} \log P_{X;\theta_0}(x) \right)^2 + O\left(\frac{1}{\sqrt{N_0}}\right) \\
&= \sum_{x \in \mathcal{X}} \left( P_{X;\theta_0}(x) + \frac{\partial P_{X;\theta_0}}{\partial \theta} (\theta_1 - \theta_0) + O\left(\frac{1}{N_0}\right) \right). \tag{46}
\end{aligned}$$

$$\begin{aligned}
& \left( \frac{\partial}{\partial \theta} \log P_{X;\theta_0}(x) \right)^2 + O\left(\frac{1}{\sqrt{N_0}}\right) \\
&= \sum_{x \in \mathcal{X}} P_{X;\theta_0}(x) \left( \frac{\partial}{\partial \theta} \log P_{X;\theta_0}(x) \right)^2 + O\left(\frac{1}{\sqrt{N_0}}\right) \tag{47}
\end{aligned}$$

$$= J(\theta_0) + O\left(\frac{1}{\sqrt{N_0}}\right) \tag{48}$$

Combining with (39) and (45),

$$(\hat{\theta} - E_{\hat{\theta}}) \xrightarrow{d} N \left( 0, \frac{N_0 + w_1^2 n_1}{(N_0 + w_1 n_1)^2} \frac{1}{J(\theta_0)} \right). \tag{49}$$

**Lemma 8.** *In the asymptotic case, the proposed measure (1) and the mean squared error have the relation as follows.*

$$\begin{aligned}
& \mathbb{E} \left[ D \left( P_{X;\theta_0} \middle\| P_{X;\hat{\theta}} \right) \right] \\
&= \frac{1}{2} J(\theta_0) MSE(\hat{\theta}) + o\left(\frac{1}{N_0}\right), \tag{50}
\end{aligned}$$

*Proof.* In this section, for the sake of clarity, we will write  $\hat{\theta}$  in its parameterized form  $\hat{\theta}(X^{N_0})$  when necessary, and these two forms are mathematically equivalent. By taking Taylor expansion of  $D \left( P_{X;\theta_0} \middle\| P_{X;\hat{\theta}(X^{N_0})} \right)$  at  $\theta_0$ , we can get

$$\begin{aligned}
& D\left(P_{X;\theta_0} \middle\| P_{X;\hat{\theta}(X^{N_0})}\right) \\
&= \sum_{x \in X} P_{X;\theta_0}(x) \log \frac{P_{X;\theta_0}(x)}{P_{X;\hat{\theta}(X^{N_0})}(x)} \\
&= -\sum_{x \in X} P_{X;\theta_0}(x) \log \frac{P_{X;\hat{\theta}(X^{N_0})}(x)}{P_{X;\theta_0}(x)} \\
&= -\sum_{x \in X} P_{X;\theta_0}(x) \log \left(1 + \frac{P_{X;\hat{\theta}(X^{N_0})}(x) - P_{X;\theta_0}(x)}{P_{X;\theta_0}(x)}\right) \\
&= -\sum_{x \in X} P_{X;\theta_0}(x) \left( \left( \frac{P_{X;\hat{\theta}(X^{N_0})}(x) - P_{X;\theta_0}(x)}{P_{X;\theta_0}(x)} \right) \right. \\
&\quad \left. - \frac{1}{2} \left( \frac{P_{X;\hat{\theta}(X^{N_0})}(x) - P_{X;\theta_0}(x)}{P_{X;\theta_0}(x)} \right)^2 \right) + o(|\hat{\theta}(X^{N_0}) - \theta_0|^2) \\
&= \frac{1}{2} \sum_{x \in X} \frac{\left( P_{X;\hat{\theta}(X^{N_0})}(x) - P_{X;\theta_0}(x) \right)^2}{P_{X;\theta_0}(x)} + o(|\hat{\theta}(X^{N_0}) - \theta_0|^2)
\end{aligned} \tag{51}$$

We denote  $\delta$  as a small constant, and we can rewrite (1) as

$$\begin{aligned}
& \mathbb{E} \left[ D\left(P_{X;\theta_0} \middle\| P_{X;\hat{\theta}(X^{N_0})}\right) \right] \\
&= \sum_{X^{N_0}} P_{X^n;\theta_0}(X^{N_0}) D\left(P_{X;\theta_0} \middle\| P_{X;\hat{\theta}(X^{N_0})}\right) \\
&= \sum_{X^{N_0}} P_{X^n;\theta_0}(X^{N_0}) \left( \frac{1}{2} \sum_{x \in X} \frac{\left( P_{X;\hat{\theta}(X^{N_0})}(x) - P_{X;\theta_0}(x) \right)^2}{P_{X;\theta_0}(x)} \right. \\
&\quad \left. + o(|\hat{\theta}(X^{N_0}) - \theta_0|^2) \right) \\
&= \sum_{X^{N_0}} P_{X^n;\theta_0}(X^{N_0}) \left( \frac{1}{2} \sum_{x \in X} \frac{\left( \frac{\partial P_{X;\theta_0}(x)}{\partial \theta_0} (\hat{\theta}(X^{N_0}) - \theta_0) \right)^2}{P_{X;\theta_0}(x)} + \right. \\
&\quad \left. o(|\hat{\theta}(X^{N_0}) - \theta_0|^2) \right) \\
&= \sum_{\{X^{N_0}: |\hat{\theta}(X^{N_0}) - \theta_0|^2 < \delta\}} P_{X^n;\theta_0}(X^{N_0}) \cdot \\
&\quad \left( \frac{1}{2} \sum_{x \in X} \frac{\left( \frac{\partial P_{X;\theta_0}(x)}{\partial \theta_0} (\hat{\theta}(X^{N_0}) - \theta_0) \right)^2}{P_{X;\theta_0}(x)} + o(|\hat{\theta}(X^{N_0}) - \theta_0|^2) \right) \\
&+ \sum_{\{X^{N_0}: |\hat{\theta}(X^{N_0}) - \theta_0|^2 \geq \delta\}} P_{X^n;\theta_0}(X^{N_0}) \cdot \\
&\quad \left( \frac{1}{2} \sum_{x \in X} \frac{\left( \frac{\partial P_{X;\theta_0}(x)}{\partial \theta_0} (\hat{\theta}(X^{N_0}) - \theta_0) \right)^2}{P_{X;\theta_0}(x)} + o(|\hat{\theta}(X^{N_0}) - \theta_0|^2) \right)
\end{aligned} \tag{52}$$

To facilitate the subsequent proof, we introduce the concept of "Dot Equal".

**Definition 9.** (Dot Equal ( $\doteq$ )) Specifically, given two functions  $f(n)$  and  $g(n)$ , the notation  $f(n) \doteq g(n)$  is defined as

$$f(n) \doteq g(n) \Leftrightarrow \lim_{n \rightarrow \infty} \frac{1}{n} \log \frac{f(n)}{g(n)} = 0, \tag{53}$$

which shows that  $f(n)$  and  $g(n)$  have the same exponential decaying rate.

We denote  $\hat{P}_{X^{N_0}}$  as the empirical distribution of  $X^{N_0}$ . Applying Sanov's Theorem to (52), we can know that

$$P_{X^n;\theta_0}(X^{N_0}) \doteq e^{-N_0 D(\hat{P}_{X^{N_0}} \parallel P_{X;\theta_0})} \tag{54}$$

Then, we aim to establish a connection between (54) and  $|\hat{\theta}(X^{N_0}) - \theta_0|^2$ . From (51), we can know that the  $D(\hat{P}_{X^{N_0}} \parallel P_{X;\theta_0})$  in (54) can be transformed to

$$\begin{aligned}
& D\left(\hat{P}_{X^{N_0}} \middle\| P_{X;\theta_0}\right) \\
&= \frac{1}{2} \sum_{x \in X} \frac{\left( \hat{P}_{X^{N_0}}(x) - P_{X;\theta_0}(x) \right)^2}{\hat{P}_{X^{N_0}}(x)} + o(|\hat{\theta}(X^{N_0}) - \theta_0|^2) \\
&= \frac{1}{2} \sum_{x \in X} \frac{\left( \hat{P}_{X^{N_0}}(x) - P_{X;\theta_0}(x) \right)^2}{P_{X;\theta_0}(x)} + o(|\hat{\theta}(X^{N_0}) - \theta_0|^2)
\end{aligned} \tag{55}$$

From the characteristics of MLE, we can know that

$$\begin{aligned}
& \mathbb{E}_{\hat{P}_{X^{N_0}}} \left[ \frac{\partial \log P_{X;\hat{\theta}(X^{N_0})}(x)}{\partial \hat{\theta}} \right] \\
&= 0 \\
&= \mathbb{E}_{\hat{P}_{X^{N_0}}} \left[ \frac{\partial \log P_{X;\theta_0}(x)}{\partial \theta_0} \right] \\
&+ \mathbb{E}_{\hat{P}_{X^{N_0}}} \left[ \frac{\partial^2 \log P_{X;\theta_0}(x)}{\partial \theta_0^2} \right] (\hat{\theta}(X^{N_0}) - \theta_0) \\
&+ O(|\hat{\theta}(X^{N_0}) - \theta_0|^2),
\end{aligned} \tag{56}$$

which can be transformed to

$$\begin{aligned}
& (\hat{\theta}(X^{N_0}) - \theta_0) + O(|\hat{\theta}(X^{N_0}) - \theta_0|^2) \\
&= -\frac{\mathbb{E}_{\hat{P}_{X^{N_0}}} \left[ \frac{\partial \log P_{X;\theta_0}(x)}{\partial \theta_0} \right]}{\mathbb{E}_{\hat{P}_{X^{N_0}}} \left[ \frac{\partial^2 \log P_{X;\theta_0}(x)}{\partial \theta_0^2} \right]} \\
&= -\frac{\mathbb{E}_{\hat{P}_{X^{N_0}}} \left[ \frac{\frac{\partial P_{X;\theta_0}(x)}{\partial \theta_0}}{P_{X;\theta_0}(x)} \right]}{\mathbb{E}_{\hat{P}_{X^{N_0}}} \left[ \frac{\partial^2 \log P_{X;\theta_0}(x)}{\partial \theta_0^2} \right]} \\
&= \frac{\sum_{x \in \mathcal{X}} (\hat{P}_{X^{N_0}}(x) - P_{X;\theta_0}(x)) \frac{\frac{\partial P_{X;\theta_0}(x)}{\partial \theta_0}}{P_{X;\theta_0}(x)}}{J(\theta_0)}
\end{aligned} \tag{57}$$

Using the Cauchy-Schwarz inequality, we can obtain

$$\sum_{x \in X} \frac{\left(\hat{P}_{X^{N_0}}(x) - P_{X;\theta_0}(x)\right)^2}{P_{X;\theta_0}(x)} \cdot \sum_x \frac{\left(\frac{\partial P_{X;\theta_0}(x)}{\partial \theta_0}\right)^2}{P_{X;\theta_0}(x)} \geq \left( \sum_{x \in \mathcal{X}} \left(\hat{P}_{X^{N_0}}(x) - P_{X;\theta_0}(x)\right) \frac{\frac{\partial P_{X;\theta_0}(x)}{\partial \theta_0}}{P_{X;\theta_0}(x)} \right)^2 \quad (58)$$

where

$$\begin{aligned} \sum_x \frac{\left(\frac{\partial P_{X;\theta_0}(x)}{\partial \theta_0}\right)^2}{P_{X;\theta_0}(x)} &= \sum_x P_{X;\theta_0}(x) \left(\frac{1}{P_{X;\theta_0}(x)} \frac{\partial P_{X;\theta_0}(x)}{\partial \theta_0}\right)^2 \\ &= \sum_x P_{X;\theta_0}(x) \left(\frac{\partial \log P_{X;\theta_0}(x)}{\partial \theta_0}\right)^2 = J(\theta_0) \end{aligned} \quad (59)$$

Combining with (55), (57), and (59), the inequality (58) can be transformed to

$$\begin{aligned} D\left(\hat{P}_{X^{N_0}} \parallel P_{X;\theta_0}\right) &= \frac{1}{2} \sum_{x \in X} \frac{\left(\hat{P}_{X^{N_0}}(x) - P_{X;\theta_0}(x)\right)^2}{P_{X;\theta_0}(x)} + o(|\hat{\theta}(X^{N_0}) - \theta_0|^2) \\ &\geq \frac{1}{2} J(\theta_0) \left(\hat{\theta}(X^{N_0}) - \theta_0 + O(|\hat{\theta}(X^{N_0}) - \theta_0|^2)\right)^2 \\ &\quad + o(|\hat{\theta}(X^{N_0}) - \theta_0|^2) \\ &= \frac{1}{2} J(\theta_0) |\hat{\theta}(X^{N_0}) - \theta_0|^2 + o(|\hat{\theta}(X^{N_0}) - \theta_0|^2) \end{aligned} \quad (60)$$

Combining (54) and (60), we can know that

$$P_{X^n;\theta_0}(X^{N_0}) \doteq e^{-N_0 D(\hat{P}_{X^{N_0}} \parallel P_{X;\theta_0})} \leq e^{\frac{-N_0 J(\theta_0) |\hat{\theta}(X^{N_0}) - \theta_0|^2}{2}} \quad (61)$$

For the first term in (52), the  $|\hat{\theta}(X^{N_0}) - \theta_0|$  is small enough for us to omit the term  $o(|\hat{\theta}(X^{N_0}) - \theta_0|^2)$ . As for the second term in (52), even though the magnitude of  $|\hat{\theta}(X^{N_0}) - \theta_0|$  is no longer negligible, the probability of such sequences is  $O(e^{\frac{-N_0 J(\theta_0) |\hat{\theta}(X^{N_0}) - \theta_0|^2}{2}})$  by (61), which is exponentially decaying with  $N_0$  such that the second term is  $o(\frac{1}{N_0})$ . By transferring (52), we can get

$$\begin{aligned} \mathbb{E}\left[D\left(P_{X;\theta_0} \parallel P_{X;\hat{\theta}(X^{N_0})}\right)\right] &= \sum_{\{X^{N_0}: |\hat{\theta}(X^{N_0}) - \theta_0|^2 < \delta\}} P_{X^n;\theta_0}(X^{N_0}) \cdot \\ &\quad \left( \frac{1}{2} \sum_{x \in X} \frac{\left(\frac{\partial P_{X;\theta_0}(x)}{\partial \theta_0} (\hat{\theta}(X^{N_0}) - \theta_0)\right)^2}{P_{X;\theta_0}(x)} \right) + o(|\hat{\theta}(X^{N_0}) - \theta_0|^2) \\ &+ \sum_{\{X^{N_0}: |\hat{\theta}(X^{N_0}) - \theta_0|^2 \geq \delta\}} P_{X^n;\theta_0}(X^{N_0}) \cdot \\ &\quad \left( \frac{1}{2} \sum_{x \in X} \frac{\left(\frac{\partial P_{X;\theta_0}(x)}{\partial \theta_0} (\hat{\theta}(X^{N_0}) - \theta_0)\right)^2}{P_{X;\theta_0}(x)} \right) + o(\frac{1}{N_0}) \\ &= \frac{1}{2} \mathbb{E}\left[\sum_{x \in X} \frac{\left(\frac{\partial P_{X;\theta_0}(x)}{\partial \theta_0} (\hat{\theta}(X^{N_0}) - \theta_0)\right)^2}{P_{X;\theta_0}(x)}\right] + o(\frac{1}{N_0}). \end{aligned} \quad (62)$$

We then transform (62) with (59)

$$\begin{aligned} \frac{1}{2} \mathbb{E}\left[\sum_{x \in X} \frac{\left(\frac{\partial P_{X;\theta_0}(x)}{\partial \theta_0} (\hat{\theta}(X^{N_0}) - \theta_0)\right)^2}{P_{X;\theta_0}(x)}\right] &= \frac{1}{2} \mathbb{E}\left[\left(\hat{\theta} - \theta_0\right)^2\right] \sum_x \frac{\left(\frac{\partial P_{X;\theta_0}(x)}{\partial \theta_0}\right)^2}{P_{X;\theta_0}(x)} \\ &= \frac{1}{2} \mathbb{E}\left[\left(\hat{\theta} - \theta_0\right)^2\right] J(\theta_0) \end{aligned} \quad (63)$$

Combining (62), (63), we can get

$$\mathbb{E}\left[D\left(P_{X;\theta_0} \parallel P_{X;\hat{\theta}}\right)\right] = \frac{1}{2} \mathbb{E}\left[\left(\hat{\theta} - \theta_0\right)^2\right] J(\theta_0) + o(\frac{1}{N_0}). \quad (64)$$

□

Finally, we make a decomposition for the K-L measure

$$\begin{aligned} \mathbb{E}\left[D\left(P_{X;\theta_0} \parallel P_{X;\hat{\theta}}\right)\right] &= \frac{1}{2} \mathbb{E}\left[\left(\hat{\theta} - \theta_0\right)^2\right] J(\theta_0) + o(\frac{1}{N_0}) \\ &= \frac{1}{2} J(\theta_0) \left(\mathbb{E}\left[\left(\hat{\theta} - E_{\hat{\theta}}\right)^2\right] + \mathbb{E}\left[\left(E_{\hat{\theta}} - \theta_0\right)^2\right]\right) + o(\frac{1}{N_0}). \end{aligned} \quad (65)$$

Substituting (27) and (49) into (65), we have

$$\begin{aligned} \mathbb{E}\left[D\left(P_{X;\theta_0} \parallel P_{X;\hat{\theta}}\right)\right] &= \frac{1}{2} \frac{N_0 + w_1^2 n_1}{(N_0 + w_1 n_1)^2} + \frac{1}{2} \frac{(w_1 n_1)^2 J(\theta_0) (\theta_0 - \theta_1)^2}{(N_0 + w_1 n_1)^2} + o(\frac{1}{N_0}). \end{aligned} \quad (66)$$

By differentiating with respect to  $w_1$ , we obtain the optimal value of weight is

$$w_1^* = \frac{1}{1 + tn_1} \quad (67)$$

Similarly, by taking the derivative of (66) with respect to  $n_1$ , we observe that the derivative is

$$-\frac{1}{2} \left( \frac{1 + n_1 t}{N_0 + n_1 + N_0 n_1 t} \right), \quad (68)$$

which is strictly negative, implying that the optimal value of  $n_1$  is  $N_1$ . Finally, we obtain the optimal value of weight in (10). □

## APPENDIX B PROOF OF PROPOSITION 3

*Proof.* Similar to (65), we can get

$$\begin{aligned} \mathbb{E}\left[D\left(P_{X;\theta_0} \parallel P_{X;\hat{\theta}}\right)\right] &= \frac{1}{2} \text{tr} \left( J(\underline{\theta}_0) \mathbb{E}\left[\left(\hat{\theta} - E_{\hat{\theta}}\right) \left(\hat{\theta} - E_{\hat{\theta}}\right)^{\top}\right] \right) \\ &\quad + \frac{1}{2} \text{tr} \left( J(\underline{\theta}_0) \mathbb{E}\left[\left(E_{\hat{\theta}} - \underline{\theta}_0\right) \left(E_{\hat{\theta}} - \underline{\theta}_0\right)^{\top}\right] \right) + o(\frac{1}{N_0}). \end{aligned} \quad (69)$$

Similar to (49), we can get

$$\left(\hat{\underline{\theta}} - E_{\hat{\underline{\theta}}}\right) \xrightarrow{d} \mathcal{N}\left(0, \frac{N_0 + w_1^2 n_1}{(N_0 + w_1 n_1)^2} J(\underline{\theta}_0)^{-1}\right). \quad (70)$$

So we can know that  $\mathbb{E}\left[\left(\hat{\underline{\theta}} - E_{\hat{\underline{\theta}}}\right) \left(\hat{\underline{\theta}} - E_{\hat{\underline{\theta}}}\right)^\top\right]$  has the limit

$$\frac{N_0 + w_1^2 n_1}{(N_0 + w_1 n_1)^2} J(\underline{\theta}_0)^{-1} \quad (71)$$

The same to Lemma 7, we can get

$$E_{\hat{\underline{\theta}}} = \frac{N_0 \underline{\theta}_0 + w_1 n_1 \underline{\theta}_1}{N_0 + w_1 n_1} + O\left(\frac{1}{N_0}\right), \quad (72)$$

Combining (69), (70) and (72), we can know that the K-L measure has the form of (11).  $\square$

## APPENDIX C PROOF OF THEOREM 5

*Proof.* Similar to (49), we can get

$$\left(\hat{\underline{\theta}} - E_{\hat{\underline{\theta}}}\right) \xrightarrow{d} \mathcal{N}\left(0, \frac{N_0 + \sum_{i=1}^K w_i^2 n_i}{\left(N_0 + \sum_{i=1}^K w_i n_i\right)^2} J(\underline{\theta}_0)^{-1}\right). \quad (73)$$

Similar to Lemma 7, we can get

$$E_{\hat{\underline{\theta}}} = \frac{N_0 \underline{\theta}_0 + \sum_{i=1}^k w_i n_i \underline{\theta}_i}{N_0 + s} + O\left(\frac{1}{N_0}\right). \quad (74)$$

Combining (69), (73) and (74), the K-L measure is

$$\frac{d}{2} \left( \frac{N_0 + \sum_{i=1}^K \frac{b_i^2}{n_i}}{(N_0 + s)^2} + \frac{s^2}{(N_0 + s)^2} \frac{\underline{\alpha}^T \Theta^T J(\underline{\theta}_0) \Theta \underline{\alpha}}{d} \right) + o\left(\frac{1}{N_0}\right). \quad (75)$$

According to (5), it is easy to observe that the optimal performance is achieved when every  $n_i$  takes its maximum value  $N_i$ . Then, we can transform (75) to

$$\begin{aligned} & \frac{d}{2} \left( \frac{N_0}{(N_0 + s)^2} + \frac{s^2}{(N_0 + s)^2} \underline{\alpha}^T \text{diag} \left( \frac{1}{N_1}, \dots, \frac{1}{N_K} \right) \underline{\alpha} \right. \\ & \left. + \frac{s^2}{(N_0 + s)^2} \frac{\underline{\alpha}^T \Theta^T J(\underline{\theta}_0) \Theta \underline{\alpha}}{d} \right) + o\left(\frac{1}{N_0}\right). \end{aligned} \quad (76)$$

$\square$

## APPENDIX D JUSTIFICATION OF THE KL-BASED MEASURE

Compared to other measures, the K-L divergence exhibits a closer correspondence with the generalization error as measured by the cross-entropy loss. In this section, we will provide a concrete example (i.e., in a classification task) where the proposed K-L divergence formulation measure aligns with the cross-entropy generalization error.

In a classification task, let  $z \in \mathcal{Z}$  denote the input features and  $y \in \mathcal{Y}$  represent the output labels. The true data-generating distribution is  $P(z, y)$ , while the joint distribution model learned from the training dataset is denoted as  $\hat{P}_{\hat{\theta}}(z, y)$ , where  $\hat{\theta}$  denotes the learnable model parameters in training. The proposed measure  $D(P \parallel \hat{P})$  is defined as follows.

$$\begin{aligned} D(P \parallel \hat{P}) &= \sum_{z \in \mathcal{Z}, y \in \mathcal{Y}} P(z, y) \log \frac{P(z, y)}{\hat{P}_{\hat{\theta}}(z, y)} \\ &= \sum_{z \in \mathcal{Z}, y \in \mathcal{Y}} P(z, y) \log P(z, y) - \sum_{z \in \mathcal{Z}, y \in \mathcal{Y}} P(z, y) \log \hat{P}_{\hat{\theta}}(y \mid z) \\ &\quad - \sum_{z \in \mathcal{Z}, y \in \mathcal{Y}} P(z, y) \log \hat{P}(z), \end{aligned} \quad (77)$$

where the second term of (77), i.e.,

$$- \sum_{z \in \mathcal{Z}, y \in \mathcal{Y}} P(z, y) \log \hat{P}_{\hat{\theta}}(y \mid z),$$

is the standard definition of generalization error in a classification task. Furthermore, the first term of (77) depends solely on the true data distribution and is constant. Though the third term involves  $\hat{P}(z)$ ,  $\hat{P}(z)$  is typically treated as a fixed marginal distribution decided by the training data rather than being learned in the model training. As a result, the third term is usually not parameterized by model parameter  $\hat{\theta}$ , and thus does not contribute to the optimization objective. In brief, the first term and the third term will not affect our optimization. Therefore, the K-L divergence formulation remains consistent with the standard definition of generalization error.